Title

DEPC modification of the CuA protein from Thermus thermophilus

Journal

JBIC Journal of Biological Inorganic Chemistry, 24(1)

ISSN

0949-8257

Authors

Devlin, Taylor
Hofman, Cristina R
Acevedo, Zachary PV
et al.

Publication Date

2019-02-01

DOI

10.1007/s00775-018-1632-y

Peer reviewed

HHS Public Access

Author manuscript

J Biol Inorg Chem. Author manuscript; available in PMC 2020 April 28.

Published in final edited form as:

J Biol Inorg Chem. 2019 February ; 24(1): 117–135. doi:10.1007/s00775-018-1632-y.

DEPC modification of the Cu_A protein from *Thermus thermophilus*

Taylor Devlin[1,4], **Cristina R. Hofman**[1], **Zachary P. V. Acevedo**[1], **Kelsey R. Kohler**[1], **Lizhi Tao**[2], **R. David Britt**[2], **Kevin R. Hoke**[3], **Laura M. Hunsicker-Wang**[1]

[1]Department of Chemistry, Trinity University, San Antonio, TX 78212-7200, USA

[2]Department of Chemistry, University of California at Davis, Davis, CA 95616, USA

[3]Department of Chemistry and Biochemistry, Berry College, Mount Berry, GA 30149, USA

[4]Present Address: Department of Biophysics, Johns Hopkins University, 3400 N. Charles Street, Baltimore, MD 21218, USA

Abstract

The Cu_A center is the initial electron acceptor in cytochrome *c* oxidase, and it consists of two copper ions bridged by two cysteines and ligated by two histidines, a methionine, and a carbonyl in the peptide backbone of a nearby glutamine. The two ligating histidines are of particular interest as they may influence the electronic and redox properties of the metal center. To test for the presence of reactive ligating histidines, a portion of cytochrome *c* oxidase from the bacteria *Thermus thermophilus* that contains the Cu_A site (the *Tt*Cu_A protein) was treated with the chemical modifier diethyl pyrocarbonate (DEPC) and the reaction followed through UV–visible, circular dichroism, and electron paramagnetic resonance spectroscopies at pH 5.0–9.0. A mutant protein (H40A/H117A) with the non-ligating histidines removed was similarly tested. Introduction of an electron-withdrawing DEPC-modification onto the ligating histidine 157 of *Tt*Cu_A increased the reduction potential by over 70 mV, as assessed by cyclic voltammetry. Results from both proteins indicate that DEPC reacts with one of the two ligating histidines, modification of a ligating histidine raises the reduction potential of the Cu_A site, and formation of the DEPC adduct is reversible at room temperature. The existence of the reactive ligating histidine suggests that this residue may play a role in modulating the electronic and redox properties of *Tt*Cu_A through kinetically-controlled proton exchange with the solvent. Lack of reactivity by the metalloproteins Sco and azurin, both of which contain a mononuclear copper center, indicate that reactivity toward DEPC is not a characteristic of all ligating histidines.

Keywords

Cu_A; Cytochrome oxidase; Diethyl pyrocarbonate; UV–visible spectroscopy; Circular dichroism; Chemical modification; Cyclic voltammetry; Electrochemistry

✉Laura M. Hunsicker-Wang, lhunsick@trinity.edu.

Electronic supplementary material The online version of this article (https://doi.org/10.1007/s00775-018-1632-y) contains supplementary material, which is available to authorized users.

Electron transport chains are integral components of both respiratory and photosynthetic processes in many forms of life. In the respiratory electron transport chain (ETC), as electrons are transferred through a series of redox centers, protons are translocated across a membrane to create an electrochemical gradient that drives the formation of ATP [1, 2]. Cytochrome *c* oxidase (Cyt*c*O) is a terminal electron acceptor, catalyzing the reduction of molecular oxygen to water while contributing to the proton motive force required for ATP synthesis. In the ba_3-type Cyt*c*O found in *Thermus thermophilus*, the Cu_A center is located in subunit II on the P (positive) side of the plasma membrane, where it accepts an electron from cytochrome *c* and transfers it to heme *b* [2]. The electron is then transferred to the heme a_3/Cu_B site where molecular oxygen is reduced to water. Four protons from the N (negative) side of the membrane are consumed as substrates in the process, and two protons (in ba_3-type oxidases) are pumped across the membrane for every four electrons delivered from cytochrome *c* [3].

The properties and redox activities of the initial electron acceptor in Cyt*c*O, the Cu_A site, are of particular interest. The Cu_A site of cytochrome *c* oxidase is located in a solvent-exposed domain of subunit II (Fig. 1). The center is made up of two copper ions bridged by two cysteines (Cys149 and Cys153 in *T. thermophilus)* and ligated by two histidines (His114 and His157), a methionine (Met160), and the peptide backbone carbonyl of a nearby glutamine (Gln151) (Fig. 1) [4–7]. When oxidized, Cu_A is in a mixed valence state; the center formally contains one Cu^{1+} and one Cu^{2+}, but the single unpaired electron is completely delocalized between the two coppers, producing a charge-delocalized $Cu^{+1.5}$–$Cu^{+1.5}$ or class III state [7, 8]. The native oxidized form of *Tt*Cu_A, the soluble portion of subunit II of the ba_3-type cytochrome *c* oxidase from *T. thermophilus*, has a purple color, a distinct axial electron paramagnetic resonance (EPR) signal with a seven-line hyperfine structure [8], and UV absorption bands at 365, 477, 530, and 790 nm [4, 7, 9]. The characteristic purple color and distinct EPR signal are lost upon reduction to a Cu^{1+}–Cu^{1+} state [5]. Cu_A sites have been successfully engineered into other blue copper proteins such as azurin from *Pseudomonas aeruginosa* (Cu_A azurin), allowing for study of the dinuclear metal center in other model systems [10]. Interestingly, the electronic properties of the Cu_A site in both *Tt*Cu_A and Cu_A azurin are pH and temperature dependent [4, 11–14]. By contrast, the *Tt*Cu_A reduction potential is resilient to changes from pH 4–7 [13] while Cu_A azurin shows a dramatic pH-dependence to its reduction potential in this same pH range [11].

To investigate the importance of the ligating histidines in controlling the electronic and redox properties of the Cu_A site, the nucleophilic reactivity of the two ligating histidines in *Tt*Cu_A was probed by exposing the protein to diethyl pyrocarbonate (DEPC) over a range of pH values. DEPC is a chemical modifier that reacts with deprotonated histidines to add a carboethoxy group to a ring nitrogen [15, 16]. Reactive histidines are defined by a nucleophilic nitrogen that is at least transiently available to react with DEPC, allowing for their modification. Previous work with the *T. thermophilus* Rieske protein from complex III of the ETC (trunc*Tt*Rp) revealed that the histidines ligating the [2Fe–2S] cluster react with DEPC and that modification with DEPC leads to reduction of the metal center, presumably due to a significant change in reduction potential upon DEPC modification [17]. Thus we sought to determine whether the ligating histidines at the Cu_A site, which is solvent-exposed, dinuclear, and involved in electron transfer like the [2Fe–2S] center in Rieske, would also be

reactive toward DEPC. A scheme for the formation of the DEPC adduct with the more solvent-exposed His157 in *Tt*Cu_A and the reversal of this reaction by a base, such as sodium hydroxide, is shown in Fig. 1. The resulting adduct can be identified spectroscopically as an increase in absorbance in the 230–250 nm range, and the number of modified histidines can be determined using the molar absorptivity of the adduct at 240 nm (ε_{240} = 3200 M^{-1} cm^{-1}) [15]. The effect of chemical modification may also be observed as changes in the visible circular dichroism (CD) spectrum. Importantly, DEPC does not exclusively react with histidines; it also known to react with tyrosines, lysines, and the N-terminus of proteins [15, 16]. *Tt*Cu_A (PDB code 2CUA) [7] has four solvent-accessible histidines, two of which, His114 and His157, are ligating the copper ions (Fig. 1). One of the remaining non-ligating histidines, His40, is not conserved, and the final histidine, His117, resides about 10 Å from the cluster. Neither non-ligating histidine is expected to influence the structure or redox properties of the Cu_A metal center.

As the initial electron acceptor in cytochrome *c* oxidase, the reduction potential and reorganization energy of the Cu_A center are fine-tuned for long-range electron transfer from cytochrome *c* to heme *a*/*b* [18–20]. Therefore, the histidines ligating this dinuclear metal center may play a role in modulating its essential electronic properties, and their susceptibility to chemical modification could elucidate this role. To probe this reactivity, varying amounts of DEPC were reacted with the *Tt*Cu_A protein and a double mutant with the two non-ligating histidines mutated to alanines (H40A/H117A). A reactive ligating histidine at the Cu_A site, as identified by successful DEPC modification, requires that the N^{ε} atom of the ligating histidine to be at least transiently deprotonated near physiological pH. The reactive histidine may indicate a location that supports proton-coupled electron transfer (PCET) in Cyt*c*O. Alternatively, a reactive ligating histidine in *Tt*Cu_A may play a role in regulating the electronic and redox properties of the metal center based on local pH fluctuations.

Experimental methods

Mutagenesis of *Tt*Cu_A, *Tt*Sco, and azurin

Mutations to the non-ligating histidines in *Tt*Cu_A, *Tt*Sco, and azurin were made using the QuikChange II site Directed Mutagenesis Kit (Agilent Technologies). All mutants and the primers used to make them are listed in Table 1. Successful PCR amplification was verified by running the PCR product on a 1% agarose gel stained with ethidium bromide. PCR products were then digested with Dpn1 and transformed into QuikChange XL1-Blue super competent cells (Agilent Technologies) according to kit instructions. Plasmids were extracted using a High Speed Plasmid Mini Kit (IBI Scientific) and sequenced to confirm the mutations.

Growth and purification of *Tt*Cu_A and mutants

The *Tt*Cu_A protein and H40A/H117A were expressed and purified as was described previously for *Tt*Cu_A [9], with a few minor changes. First, the expression plasmid contained an ampicillin resistance gene instead of a kanamycin gene, and is the parent plasmid used previously to study *Tt*Sco function [21]. Secondly, the sample regularly needed further

purification after the CM column. When necessary, the sample was further purified over an SHP cation exchange column (HiTrap SP HP 5 mL column, GE Healthcare) on an FPLC at 4 °C equilibrated with 50 mM sodium acetate, 0.02% Tween, pH 4.6 and eluted with 50 mM sodium acetate, 1 M NaCl, 0.02% Tween, pH 4.6 at a 14% gradient. The purity was verified using a 12% Bis–Tris SDS-PAGE gel (Invitrogen). Impure fractions were further purified over a HiLoad 16/600 Superdex 75 size-exclusion column (GE Healthcare) equilibrated and eluted with 50 mM sodium acetate, 100 mM NaCl, pH 4.6. Final purity was verified with a SDS-PAGE gel. Samples were quantified using the Edelhoch method [22, 23] and stored at −20 °C.

Growth and purification of *Tt*Sco and mutants

pET30 plasmids containing kanamycin resistance and His-tagged *Tt*Sco or H6A/H100A were grown and purified as was described for other *Tt*Sco mutants previously [21], except that MMTS was not added to the lysis mixture to cap the thiols. The proteins were quantified using the Edelhoch method [22, 23].

To make the holo Sco protein, copper was anaerobically added to the apo protein after purification. In an anaerobic glove bag, the protein was reduced with a 10× molar excess of dithiothreitol (DTT) for an hour then run over a PD-10 column (GE Healthcare) to remove the DTT. $CuSO_4$ was added anaerobically in a 1:1.1 mol ratio of protein to Cu^{2+}, and the formation of holo *Tt*Sco was confirmed by the appearance of a pale pink color and a peak centered at 358 nm in the UV–visible spectrum.

Growth and purification of azurin

Azurin from *Pseudomonas aeruginosa* was expressed in *E. coli* and then purified in a manner similar to that described elsewhere [24, 25]. Briefly, BL21(DE3) *E. coli* cells were transformed with a pET-9a vector, originally from the laboratory of the late Professor John H. Richards, containing a gene encoding azurin from *Pseudomonas aeruginosa*. Peri-plasmic expression was used so that the azurin could be obtained using an osmotic shock procedure [24]. The resulting periplasmic factions were treated with sodium acetate to 25 mM at pH 4.5 to precipitate less stable impurities and then $CuSO_4$ was added to a final concentration of 5 mM. Upon addition of the copper, the azurin solution turned a deep blue color. The azurin solution was centrifuged to remove any remaining precipitate.

The azurin was dialyzed into 25 mM sodium acetate at pH 4.5 and then purified on a CM Sepharose Fast Flow cation exchange column (bed volume of 15 mL, GE Healthcare) equilibrated with 25 mM sodium acetate, pH 4.5 and eluted with 25 mM sodium acetate, 50 mM NaCl, pH 4.5. Azurin can also bind adventitious zinc ions during isolation of apo azurin. To remove any Zn-bound azurin, the protein was dialyzed into 15 mM sodium acetate at pH 4.5 and then the Cu-azurin was reduced using excess sodium dithionite. The protein was then purified using a SHP cation exchange column (HiTrap SP HP 5 mL column, GE Healthcare) on a FPLC at 4 °C and eluted using a 50% gradient from 15 to 300 mM sodium acetate buffer. The fractions for the first of two chromatographic peaks contained copper(I) azurin and were collected and re-oxidized with potassium ferricyanide, restoring the blue color. Purity was assessed using an SDS-PAGE gel and UV–visible

spectroscopy, for which the desired A_{628}/A_{280} ratio was greater than or equal to 0.6. Concentrations were determined using the UV–visible absorbance and the molar absorptivity at 628 nm (ε_{628} = 5900 M^{-1} cm^{-1}) [26]. Pure samples were dialyzed into 25 mM sodium phosphate buffer at pH 8.0 prior to spectroscopic experiments using DEPC. For the H35A/H83A and H35A/H83A/F114A azurin mutants, all purification steps were identical except that the acetate buffers were at pH 4.1.

UV–visible spectroscopy of DEPC modification reactions

UV–visible data was collected on a Hitachi UV–visible 2900 spectrophotometer. Cu_A samples were dialyzed in 25 mM sodium phosphate buffer at pH 6.0, 7.0, 8.0, or 9.0 or in 25 mM sodium acetate buffer at pH 5.0. Experiments with Sco were performed in 10 mM sodium phosphate, 0.05% Tween buffer at pH 7.0, and azurin was dialyzed into 25 mM sodium phosphate buffer at pH 8.0. All samples were diluted to 500 μL of 40 μM protein. An initial spectrum was taken before the addition of 1, 3, 5, 10, 20, 100 or 400 equivalents of DEPC. The neat DEPC is 6.79 M and dilutions were made in 200 proof ethanol (400 equivalents of DEPC is at or near a saturating amount of DEPC in aqueous buffer) such that the added volume was no more than 5 μL. Measurements were recorded every nanometer from 200 to 800 nm every 2 min for 40 min post addition of DEPC. All experiments were done in triplicate at 25 °C. The estimated number of DEPC modified histidines per protein molecule was calculated using the change in absorbance at 240 nm and the molar absorptivity of the DEPC-histidine adduct (ε_{240} = 3200 M^{-1} cm^{-1}) [15]. The estimated number of modified histidines was then plotted against the corresponding equivalents of DEPC (Eq. DEPC) and the resulting curve fit to find the total number of DEPC modifiable histidines (T_{DEPC}) and the number of equivalents of DEPC needed to reach one-half of the total number of modifiable histidines (K_{DEPC}), using Eq. 1:

$$\text{Number of Modifiable Histidines} = \frac{(T_{DEPC}) \times (\text{Eq.DEPC})}{K_{DEPC} + \text{Eq.DEPC}} \quad (1)$$

Circular dichroism spectroscopy of DEPC modification reactions

Circular dichroism experiments were performed on a Jasco J-815 spectropolarimeter. The initial spectrum from 300 to 700 nm of each sample of 200 μM *Tt*Cu_A in 25 mM sodium phosphate buffer at pH 6.0, 7.0, 8.0, or 9.0 or in 25 mM sodium acetate buffer at pH 5.0 was recorded. After the addition of DEPC, scans were taken from 300 to 700 nm every 2 min for 30 min. Far UV CD scans of 20 μM protein were recorded from 200 to 260 nm every 5 min for 30 min after the addition of DEPC. For *Tt*Sco, the spectrum of 100 μM holo protein at pH 7.0 was recorded from 250 to 700 nm every 2 min for 90 min after the addition of DEPC. Azurin samples at pH 8.0 and a concentration of 100 μM were also monitored from 250 to 700 nm with a spectrum recorded every 2 min for 90 min after the addition of DEPC. All experiments were performed in triplicate at 25 °C.

To investigate the reversibility of the DEPC-histidine adduct in *Tt*Cu_A, DEPC-modified samples at pH 6.0 and 8.0 were left at room temperature for 48 h. CD spectra were obtained at 2, 4, 6, 18, 24, and 48 h after the addition of DEPC.

Electron paramagnetic resonance

TtCu_A and H40A/H117A were dialyzed into 25 mM sodium phosphate buffer at pH 7.0 and concentrated to a final protein concentration of nearly 1 mM. Modified samples were prepared by treatment with 400 equivalents of DEPC. Both modified and unmodified samples were cryoprotected with 30% (v/v) glycerol and stored at −80 °C until use. The X-band (9.38 GHz) continuous-wave (CW) EPR spectra were recorded on a Bruker (Billerica, MA) EleXsys E500 spectrometer equipped with a super-high Q resonator (ER4122SHQE). Cryogenic temperatures were achieved and controlled using an ESR900 liquid helium cryostat in conjunction with a temperature controller (Oxford Instruments ITC503) and gas flow controller. CW EPR data were collected under slow-passage, non-saturating conditions. The spectrometer settings were as follows: conversion time = 40 ms, modulation amplitude = 0.5 mT, and modulation frequency = 100 kHz; other settings are given in corresponding figure captions. Simulations of the CW spectra and the following pulsed EPR spectra were performed using EasySpin 5.1.10 toolbox [27, 28] within the Matlab 2014a software suite (The Mathworks Inc., Natick, MA, USA).

Electrochemical measurements

Gold working electrodes (2 mm-diameter gold surface) were polished with 0.3 μm aluminum oxide powder in deionized water (resistivity of 18.2 Ω cm) and then ultra-sonicated in deionized water for 0.5–1 min. This process was then repeated using 0.05 μm aluminum oxide powder. The electrodes were then subjected to electrochemical cycling in 0.1 M H_2SO_4 over a range of 0.6–1.85 V vs. the standard hydrogen electrode (SHE) to prepare the surface as described elsewhere [29]. Electrodes were rinsed with deionized water, then absolute ethanol, and then incubated overnight in parafilm-sealed vials containing 10 mM 3-mercapto-1-propanol in ethanol to form a self-assembled monolayer capable of interacting with protein at the gold surface.

The thiol-prepared gold electrode was rinsed with 2–3 mL ethanol, then 2–3 mL of deionized water. A 10-μL sample of protein solution (160 μM *Tt*Cu_A in 25 mM sodium phosphate buffer, pH 8.0) was micropipetted onto the electrode surface before a Pierce minidialysis cup (3000 MWCO) was placed over the tip of the electrode. This approach for using small sample volumes in an otherwise typical electrochemical cell has been described elsewhere [30]. However, volumes this small also require tapering of the working electrode body to 6.2 mm to reach the dialysis membrane. Working electrodes (CH instruments) were carefully sanded to achieve the necessary diameter. Also, any superfluous extruded plastic in the interior of the dialysis cup was trimmed to facilitate insertion of the electrode into the cup.

The working electrode was placed in a glass vial containing degassed buffer solution (under argon gas) along with a platinum wire as the counter electrode and a saturated calomel electrode (SCE) as a reference. All electrode potentials reported here were converted to the SHE using the relationship $E_{SHE} = E_{SCE} + 243$ mV at 22 °C [31]. The electrochemical cell was placed within a grounded Faraday cage and cyclic voltammetry and square wave voltammetry were obtained using a CH Instruments electrochemical workstation. Baseline correction and peak fitting were carried out using SOAS software [32].

The same voltammetric measurements were repeated for a sample in which *Tt*Cu_A was mixed with 20 equivalents DEPC. For this modification reaction, a 3.2-M stock solution of DEPC in absolute ethanol was diluted 100-fold in buffer, and then a small volume of this solution was added promptly to the protein solution to give the desired 20:1 ratio of DEPC to *Tt*Cu_A. Voltammetry was carried out on 10 μL of this sample as soon as practical after mixing (approximately 1 min) and then repeated at increasing time intervals. After 50 min, a new 10 μL aliquot from the reaction mixture of DEPC and *Tt*Cu_A was examined using a fresh electrode.

Solvent accessibility calculations using GetArea

For all proteins used in this work, the solvent accessibility of the histidine residues was determined using the GetArea program [33]. In each case, previously determined structures were used: 2CUA [7] for holo *Tt*Cu_A, 2LLN [34] for apo *Tt*Cu_A, 2K6 V [35] for *Tt*Sco, 1AZU [36] for wild type azurin, 1AZN [37] for F114A azurin, 3FOU [38] for trunc*Tt*Rp, Human Cu(I)-Sco 2GT6 [39], Human Zn(II)-Sco 2GQL [39], and Yeast Cu(I)-Sco 2B7J [40]. For apo *Tt*Cu_A and *Tt*Sco and the Zn(II)- and Cu(I)-bound Human Sco, solution structures from NMR measurements were used, while the others were obtained from X-ray crystallography. For the NMR structures, each individual model was put into a separate PDB file which was then submitted to the program.

Results

DEPC Modification of *Tt*Cu_A and H40A/H117A observed by UV–visible spectroscopy

To highlight the reactivity of the ligating histidines in *Tt*Cu_A, a mutant H40A/H117A protein was created to remove the non-ligating histidines. Both *Tt*Cu_A and H40A/H117A were treated with 400 equivalents of DEPC in different pH conditions, and each reaction was monitored over 40 min using UV–visible spectroscopy. Following the reaction at pH values between 5.0 and 9.0 allowed assessment of the effect of pH on modification. Representative difference spectra of *Tt*Cu_A and H40A/H117A upon treatment with DEPC at pH 7.0 are shown in Fig. 2a, b. Difference spectra at all pH values clearly showed an increase in absorbance near 240 nm, indicating DEPC modification (Supplement Figs. S1 and S2). Small differences were also observed in the charge-transfer bands, particularly near 480 nm, in addition to a decrease in absorbance at 280 nm.

The number of histidines modified in each trial was estimated using the molar absorptivity of the DEPC-histidine adduct formed in the presence of free histidine (ε_{240} = 3200 M^{-1} cm^{-1}) [15] and the change in the UV–visible absorbance after 40 min of reaction time. The estimated number of modified histidines for both the *Tt*Cu_A and H40A/H117A at each pH is summarized in Table 2. At pH 7.0 the average number of modified histidines in *Tt*Cu_A is approximately three while in the double mutant only one histidine is modified. In combination, the data suggest that one ligating histidine is modified in both cases and that, when present, the two non-ligating histidines are also modified by DEPC. In comparing the UV–visible spectra at pH 7.0, the change in absorbance is clearly greater for the wild-type protein, a fact that parallels the larger number of histidines available for modification (Fig. 2a–b). Additionally, all four histidines appear to be fully modified when apo-*Tt*Cu_A is

reacted with DEPC (Table 2). The absence of the copper ions exposes the N^{δ} atoms on each histidine and must give DEPC access to the normally buried His114. Consistent with this, the solution structure for apo-*Tt*Cu_A does show a small solvent exposure for this residue (vide infra). The calculation of the number of modified histidines is only a rough estimation. The molar absorptivity value was originally calculated using free histidine in solution, and it does not account for other products such as double modifications of a single histidine and ring-openings induced by DEPC modification [41, 42]. Additionally, these values may be slightly overestimated due to residual apo protein in the samples and because we have found that DEPC itself has a small absorbance at 240 nm (ε_{240} = 0.7 M^{-1} cm^{-1}, Supplement Fig. S3).

Completion of the DEPC-modification experiments at a range of pH values revealed the pH-dependence of histidine reactivity. For *Tt*Cu_A at all pH values, the reaction appears to reach completion within the first 10 min as the absorbance difference at 240 nm remains constant beyond this time point (Fig. 2c; Supplement Fig. S1a–e). In general, the rate of reaction increases with increasing pH, most likely due to the increased availability of nucleophilic nitrogen atoms on reactive histidines. At higher pH (pH 7.0–9.0), the maximum absorbance difference occurred 2 min after the addition of DEPC. After 2 min, the 240-nm absorbance difference decreased before leveling out (Fig. 2c). This unexpected result may be explained by the removal of the DEPC-histidine of adduct in the presence of hydroxide [15, 17]. However, examination of the full spectrum over time also reveals a pH-dependent decrease in absorbance at 280 nm, which becomes more prominent as pH increases from 7.0 to 9.0. This secondary spectral change at 280 nm suggests tyrosine modification as another cause of the smaller, delayed decrease in absorbance at 240 nm observed at higher pH values (Supplement Fig. S1a–e). A similar pH-dependence was obtained for H40A/H117A, (Fig. 2b; Supplement Fig. S2aμe), though the DEPC reaction is qualitatively slower at pH 5.0–7.0 when compared to the wild-type protein. Additionally, the absorbance at 280 nm decreased throughout the 40 min of observation for modification of the mutant at pH values between 7.0 and 9.0, which parallels the pH-dependence of absorbance changes at 280 nm seen in *Tt*Cu_A.

DEPC modification of *Tt*Cu_A and H40A/H117A observed by circular dichroism spectroscopy

Further evidence of a modified ligating histidine is the change to the circular dichroism (CD) spectrum in the visible region after the addition of 400 equivalents of DEPC. Changes to the visible region of the CD spectrum, 300–700 nm, indicate electronic or structural changes to the metal center, presumably due to modification of a ligating histidine. The observed changes to the *Tt*Cu_A and H40A/H117A CD spectra upon addition of DEPC include increases in the signal at 440 nm and a peak that is red-shifted from 550 nm to 580 nm (Fig. 3; Supplement Fig. S4). Clear changes in the spectra are observed when DEPC is added to H40A/H117A at pH 6.0–9.0, but at pH 5.0 no changes occur within 40 min of reaction. By specifically comparing the changes at 440 nm (Fig. 3f), the pH-dependence of the reaction again becomes clear. The amount and rate of change becomes more dramatic with increasing pH, which parallels the spectral changes observed when *Tt*Cu_A is modified by DEPC (Supplement Fig. S3). Because the same changes to the CD spectrum are seen in both

proteins, they are very likely caused by DEPC modification of a ligating histidine, which is consistent with the UV–visible data. Structural changes induced by modification of shared tyrosines or lysines cannot be ruled out, but the far UV CD spectra from 200 to 260 nm of both *Tt*Cu_A and H40A/H117A experience only small perturbations upon the addition of DEPC. The prominent β-sheet contribution remains unchanged, indicating that the cupredoxin fold is maintained (data not shown).

Fewer equivalents of DEPC

At higher pH, the reaction of histidines in *Tt*Cu_A with DEPC occurs within 2 min, indicating that the histidines are highly reactive toward this small molecule. To systematically investigate the reactivity of these histidines, the Cu_A proteins were treated with 1, 3, 5, 10, 20, 100, and 400 equivalents of DEPC at pH 8.0 and observed using UV–visible spectroscopy (Fig. 4; Supplement Figs. S5 and S6).

For *Tt*Cu_A, as the concentration of DEPC was increased, the change in absorbance at 240 nm increased steadily, achieving a maximum change when reacting with 400 equivalents (Fig. 4a). For H40A/H117A, the maximum change in absorbance at 240 nm was reached using as few as five equivalents of DEPC (Fig. 4b). The number of modified histidines from each reaction was plotted against the equivalents of DEPC to generate saturation curves (Fig. 4c), which were fit according to Eq. 1 (see “Experimental Methods”). The fit predicts a maximum of 2.7 histidines modified for *Tt*Cu_A and 0.6 histidines for H40A/H117A. The number of DEPC equivalents needed to reach half-saturation is 4.2 for *Tt*Cu_A and 3.1 for H40A/H117A (Fig. 4c).

For both proteins, the characteristic changes to the visible CD spectrum are not observed using 1 equivalent of DEPC but are seen when as few as five equivalents of DEPC are added to the protein (Fig. 5). For such a small amount of DEPC to produce spectral change in the visible region, the ligating histidine(s) must be highly reactive compared to most other histidine, tyrosine or lysine residues. For CD spectra obtained using the full range of DEPC equivalents, see Supplemental Figs. S7 and S8 for *Tt*Cu_A and H40A/H117A, respectively.

Time-dependent removal of the DEPC-histidine adduct

Because hydroxide promotes the hydrolysis of the DEPC-histidine adduct to release ethanol and CO_2 [43], DEPC modifications occurring at higher pH are more readily removed. To test this release in *Tt*Cu_A, protein at pH 8.0 was reacted with 400 equivalents of DEPC at room temperature and then monitored by CD spectroscopy over the course of 48 h. The spectrum changed within 2 min of adding the DEPC, and all the initial changes persisted for at least 6 h. However, at 18 h after the addition of DEPC, the characteristic increase at 440 nm began to reverse, and the absorbance at this wavelength completely reverted to its original absorbance after 48 h of reaction at room temperature (Fig. 6). Interestingly, not all changes to the spectrum are completely reversed. While the increase at 440 nm and the shift at 550 nm revert to their original places, changes at 330, 490, and 590 nm do not. The same CD reversibility experiment was repeated at pH 6.0, and the change at 440 nm was again reversible over 48 h, indicating that the adduct is still removed at lower pH values. The transitions that did not revert at pH 8.0, in particular the increase in absorbance at 490 nm,

did return to their original absorbance values when the reactions were performed at pH 6.0 (Supplement Fig. S9).

DEPC modification of *Tt*Cu_A observed by voltammetry

Voltammetry of protein samples was carried out on 10-μL samples, using commercially available dialysis cups to trap the sample at the surface of the gold electrode [30]. Cyclic voltammetry of *Tt*Cu_A gave reversible oxidation–reduction signals centered at a potential of 266 mV vs. SHE at pH 8.0 (Fig. 7a, solid curve), comparable with values reported elsewhere [13, 44]. Voltammetry was then performed on a sample of *Tt*Cu_A that had been mixed with 20 equivalents of DEPC. Even after just 1 min of reaction, broadened shoulders and shifting of the voltammetric peaks indicated the presence of a new electroactive species at a potential higher than that for unmodified Cu_A (Fig. 7b). Over a period of 50 min, the peak positions stabilized somewhat, but there was an overall loss of current, likely due to the presence of adsorbed protein on the electrode. Control experiments revealed that using electrodes with *Tt*Cu_A at these concentrations (140–160 μM) for such prolonged periods of time resulted in some weak adsorption of *Tt*Cu_A. Small peaks due to adsorbed *Tt*Cu_A were present in the voltammograms when the protein sample was removed from the electrode, which was then immersed in a separate vial of buffer for a few minutes before being returned to the electrochemical cell (Supplement Fig. S10). In general, the best voltammetric responses were obtained using fresh electrode surfaces for each scan.

The reaction of *Tt*Cu_A with DEPC was allowed to proceed for 40–50 min, and then voltammetry was carried out on another 10 μL sample of the reaction mixture using a fresh electrode of the same preparation as before. The resulting voltammetry showed a clear signal at 339 mV vs. SHE, with a strong current response (Fig. 7a, dashed curve). This upshift in potential upon DEPC-modification is consistent with the addition of an electron-withdrawing group at the active site. For this sample, the presence of unmodified protein was not observed by either cyclic voltammetry or by the more sensitive technique of square wave voltammetry (data not shown). However, the width of the voltammetric signals makes it difficult to rule out entirely the presence of small contributions due to unmodified protein at the edge of the peaks for the DEPC-modified protein. Adsorption of DEPC-Cu_A to the electrode surface was much less than for *Tt*Cu_A. The DEPC-treated *Tt*Cu_A sample was examined again after 24 and 72 h storage at 5 °C (Fig. 7c). Broadening of the peaks, notably towards lower potential, was consistent with partial loss of the DEPC-modification due to hydrolysis over time. Similar results were observed for H40A/H117A (data not shown).

Buffer solutions containing DEPC, but not *Tt*Cu_A, were also examined over the same range of potentials and no oxidation or reduction processes were observed. To be completely certain of our assignment of the voltammetric response, we also prepared samples of free histidine, free lysine, and free tyrosine and treated them with DEPC (data not shown). No oxidation–reduction processes were observed for these samples either, indicating that the signal observed for DEPC-modified *Tt*Cu_A arises from oxidation and reduction at the copper site, and not from DEPC alone nor from a free DEPC-amino acid adduct.

Voltammograms for samples with significant contributions from modified and unmodified *Tt*Cu_A were examined in more detail. The square wave voltammograms were much simpler

to deconvolve than the corresponding cyclic voltammograms since the method of square wave voltammetry subtracts most of the background current response [31]. Square wave voltammograms were treated to additional baseline correction and then modeled as two overlapping Nernstian peaks, one at the potential of *Tt*Cu_A and the other at the potential of DEPC-Cu_A (Supplement Fig. S11). The area of each modeled peak corresponds to the relative abundance of each protein. One caveat for this approach is that voltammetric responses are also dependent on the interfacial electron transfer rate. However, the peak separations at scan rates > 1 V/s in the cyclic voltammetry were very similar for both DEPC-Cu_A and unmodified *Tt*Cu_A, which suggests very similar interfacial electron transfer rates. From the relative contributions of each signal, we estimated that 16% and 44% hydrolysis of DEPC-Cu_A occurred after 24 and 72 h, respectively, at pH 8.0 and 5 °C.

DEPC modification of *Tt*Cu_A and H40A/H117A observed by electron paramagnetic resonance spectroscopy

Both modified and unmodified *Tt*Cu_A were monitored using electron paramagnetic resonance (EPR) spectroscopy (Fig. 8). The collected spectra matched the expected axial signal with a seven-line hyperfine structure characteristic of the Cu_A site and were best fit with g = (2.185, 2.055, 2.320) and ACu = (90, 30, 30) MHz [8]. The DEPC-modified protein showed only small changes in the spectrum, including a slight broadening of the signal and decreased intensity of some hyperfine structure. The g values and splitting constants remained unchanged. The minor changes in EPR signals after modification indicate that the cluster was not reduced during DEPC modification, which is consistent with UV–visible and CD data, and that any DEPC-induced differences must be subtle. Similar trends are observed in comparing modified and unmodified H40A/H117A (Fig. 8b).

DEPC modification of *Tt*Sco and H6A/H100A

Histidines that are reactive to DEPC have been found in the *Thermus thermophilus* Rieske protein [17] and now the *Tt*Cu_A protein. These two systems both contain dinuclear centers, and thus it may be possible that these types of clusters promote such reactivity. To test the importance of a dinuclear metal center and the role of solvent accessibility of the ligands in determining the reactivity of ligating histidines, two proteins containing a mononuclear copper site were also subjected to the same DEPC assays. The first of these is Sco from *T. thermophilus* (*Tt*Sco) (Fig. 9a). Sco has been proposed to assist in the formation of the Cu_A site in Cyt*c*O by reducing the disulfide bond in apo *Tt*Cu_A before the insertion of copper, though Sco's exact function is still debated and may vary across species [21, 35, 39, 45–49]. It binds one copper ion, which is ligated by two cysteines and one histidine (Fig. 9b) [35]. The UV–visible spectrum of holo *Tt*Sco has a ligand-to-metal charge-transfer band at 358 nm and less intense peaks at 466 and 560 nm, making it a red copper site [35, 50]. As a metalloprotein containing a histidine-ligated copper center, the mononuclear *Tt*Sco center shares some structural features with the dinuclear *Tt*Cu_A center. Like *Tt*Cu_A, nothing in the literature suggests that the ligating histidine His139 in *Tt*Sco is readily ionizable and thus predisposed to react with DEPC.

While the solvent accessibility of His139 in holo *Tt*Sco is not known, its accessibility in a solution structure for apo *Tt*Sco was 12.6% (Table 3), as determined using GetArea [33]. For

comparison, a minimized average solution structure for human Cu(I)-Sco has a ligating histidine with 6.9% accessibility, whereas the corresponding accessibility in an NMR solution structure of human Ni(II)-Sco is only 1.9% [39]. A yeast Cu(I)-Sco crystal structure with a disordered copper site that does not contain the conserved cysteines and histidines of other Sco proteins contains a ligating histidine with 37% accessibility [40]. Although the actual solvent accessibility of Cu(II)-*Tt*Sco is unknown, if modification of a ligating histidine in *Tt*Sco occurs, it would suggest that it is more solvent-accessible than the corresponding histidine in human Sco and that reactivity toward DEPC is a general property of solvent-exposed ligating histidines.

Holo *Tt*Sco was reacted with 400 equivalents of DEPC at pH 7.0, and the reaction was monitored by UV–visible spectroscopy. An increase in absorbance was observed at 240 nm, and the magnitude of change indicated that only one histidine is modified by DEPC, probably the non-ligating His6 based on the solvent accessibility (55.8%) (Fig. 9c, Table 3). When monitoring the reaction using CD spectroscopy in the visible region, a minimal degree of change to the spectrum was observed over the course of 2 hours (Fig. 9d), and the loss of signal intensity is comparable to that seen in unmodified holo *Tt*Sco left at room temperature for multiple hours (Supplement Fig. S12). A double mutant, H6A/H100A, was made to remove all but the ligating histidine (His139). For this double mutant, there was still a small increase in absorbance near 240 nm equivalent to 0.4 modified histidines. However, the maximum difference in absorbance does not occur at 240 nm but is shifted to 247 nm (Fig. 9e). Therefore, the number of modified histidines was estimated using the absorbance change at 247 nm and the molar absorptivity value of 3200 M^{-1} cm^{-1}. For comparison, free DEPC alone has a small absorbance in the 230–250 nm range equivalent to that for 0.1 modified histidines at these concentrations. The visible CD spectrum of H6A/H100A does not change significantly after the addition of DEPC. All spectral features decrease slightly and consistently in intensity, suggesting that the changes are not due to DEPC modification (Fig. 9f). Taken together, these results are suggestive of some copper loss, and DEPC modification of the apo protein. In the UV–visible spectra, both wild-type and H6A/H100A *Tt*Sco proteins decreased in absorbance at 280 nm after the addition of DEPC, and the magnitude of this change was consistent across both proteins, suggesting that some other residue, possibly a tyrosine, is equally modified in both.

DEPC modification of azurin

Another copper-containing electron transfer protein examined was the blue copper protein azurin from *Pseudomonas aeruginosa* (Fig. 10a). Located in the periplasm of bacteria, azurin transfers electrons from cytochrome c_{551} to nitrite reductase as part of the denitrification pathway [51]. The protein contains a type 1 copper center with a ligation environment similar enough to Cu_A that a Cu_A site can be engineered into the azurin protein scaffold [10, 11, 52]. Two histidines, one cysteine, and one methionine, ligate one copper ion in azurin (Fig. 10b). The UV–visible absorption spectrum contains one major peak in the visible region, and an intense charge-transfer band at 628 nm corresponding to a S(Cys)→Cu transition [53]. Because the metal ligation environment, spectroscopic characteristics, and functional properties are comparable in azurin and Cu_A, the ligating histidines in azurin may be equally reactive to DEPC. However, a previous report on the chemical modification of

azurin found that only a non-ligating histidine was modified, presumably due to low solvent accessibility of the ligating histidines [54].

Azurin was treated with 400 equivalents of DEPC at pH 8.0, and the reaction was observed using both UV–visible spectroscopy and visible CD spectroscopy. After the addition of DEPC, UV–visible absorbance increased at 240 nm (Fig. 10c). The change occurred within the first 2 min of reaction and corresponded to one modified histidine, most likely His83 based on its large solvent accessibility (43.6%) (Table 3). The CD spectrum from 300 to 700 nm underwent minimal change after the addition of DEPC (Fig. 10d). We also created mutants of azurin to remove the non-ligating histidines (H35A/H83A) and to increase solvent accessibility of the histidine ligand His117 (F114A). The F114A mutation removes a bulky phenylalanine residue blocking solvent access to the metal center. A triple mutant (H35A/H83A/F114A) was also created to probe the effect of these mutations in combination. Even though it increases the solvent accessibility of the ligating histidine somewhat, F114A also only had one histidine modified, suggesting that the same non-ligating histidine is modified in both F114A and wild-type azurin (Fig. 10e). The UV–visible absorbance at 240 nm increased slightly in the double and triple mutants that lacked non-ligating histidines, but this can be attributed to the presence of DEPC in solution, suggesting that no histidine modification occurs in these mutants (Fig. 10f).

Discussion

As the initial electron acceptor in Cyt*c*O, the Cu_A site plays a central role in cellular respiration. To quickly and efficiently transfer electrons from cytochrome *c* to heme *a*/*b*, the reduction potential and reorganization energy of this dinuclear metal center must be tightly controlled, and both the primary metal ligands and the overall protein matrix likely contribute to this regulation [18–20]. This study used diethyl pyrocarbonate as a chemical modifier to demonstrate that a histidine ligating the Cu_A site in *Tt*Cu_A can undergo the transient proton exchange necessary for chemical modification. Spectroscopic results indicate that one ligating histidine and both non-ligating histidines are modified by DEPC near pH 7.0. Modification of this ligating histidine alters the electronic structure of the dinuclear center, as evidenced by changes to the CD spectrum in the visible region, and raises the reduction potential by over 70 mV. The modified ligating histidine is mostly likely His157, which is the more solvent-exposed ligating histidine in holo *Tt*Cu_A and sits at the interface of the inner membrane and the periplasmic space within Cyt*c*O. Therefore, His157 is ideally situated to exchange protons with the solvent and react with DEPC.

Ligating histidine modification was observed spectroscopically in both Cu_A proteins and an increase in reduction potential was observed for *Tt*Cu_A. The upshift in potential of 73 mV following DEPC modification is consistent with introduction of the electron-withdrawing carboethoxy group onto the ligating His157 of the active site. The DEPC-modification must serve to pull electron density from the copper cluster, making reduction more favorable, resulting in the higher observed potential. On the other hand, DEPC is polar, and the presence of a polar group like the DEPC-adduct would favor the greater charge magnitude of oxidized *Tt*Cu_A, for which the net charge of the two copper atoms and two thiolate ligands is +1 compared to 0 for reduced Cu_A. However, the influence of DEPC polarity will be offset

by the decrease in accessibility of His157 to the more polar solvent (water) following this modification. Despite the increase in eduction potential, the protein remained oxidized, unlike in trunc*Tt*Rp where ligating histidine modification is accompanied by reduction of the metal center [17]. The spectroscopic changes and reduction potential increase resulting from DEPC modification of $TtCu_A$ suggest that His157 is a reactive ligating histidine.

There is significant spectroscopic evidence for modification of a ligating histidine, but modification of tyrosines and lysines may contribute to the altered CD spectra of $TtCu_A$ and H40A/H117A through structural alterations of the proteins. As primary amines, lysines are often the most reactive residues toward DEPC [55]; however, all lysines in $TtCu_A$ are located approximately 20 Å or further from the metal center, making lysine modification highly unlikely to influence metal center properties except through large-scale conformational changes. Large conformational changes are not observed as the far UV-CD spectrum of $TtCu_A$ only shifts slightly after the addition of DEPC (data not shown), effectively ruling out lysine modification as the cause of the visible CD spectral changes and the increase in reduction potential. The pH-dependent decrease in absorbance at 280 nm observed in the UV–visible spectra of both Cu_A proteins and both Sco proteins is indicative of tyrosine modification [15, 56]. This decrease in absorbance at 280 nm was also seen in an experiment where free tyrosine was mixed with DEPC and monitored by UV–visible spectroscopy (data not shown and Ref. [15]).

Decreasing the equivalents of DEPC used reveals the degree of histidine reactivity. With fewer DEPC molecules available to react with protein residues, only the most accessible and reactive amino acids are likely to form a DEPC adduct. In both $TtCu_A$ and H40A/H117A, complete DEPC-histidine adduct formation is observed using less than 10 equivalents of DEPC. In the wild-type protein, the maximum spectral change is only achieved using 400 equivalents of DEPC, but just 5 equivalents of DEPC are needed to induce the largest spectral changes at 240 nm for the H40A/H117A mutant. For both $TtCu_A$ and H40A/H117A, the same changes to the visible CD spectrum that occur when using 400 equivalents of DEPC are also observed with only 5 equivalents of DEPC. These CD results indicate that the ligating histidine is reactive toward as few as 5 equivalents of DEPC, and, therefore, the reactive ligating histidine is one of the most reactive residues in the protein. It is not unprecedented that a ligating histidine is one of the residues most susceptible to DEPC modification. Analysis of the *Thermus thermophilus* Rieske protein using mass spectrometry showed that the ligating histidine His154 is one of the first amino acids modified by DEPC [55]. Together these cases indicate that ligating histidines can be extremely reactive toward DEPC, comparable even to non-ligating histidines and lysines.

A complication to the DEPC-modification of histidines is that the DEPC-histidine adduct hydrolyzes over time [15, 43]. The results of the visible CD experiments at pH 6.0 and 8.0 indicate that the DEPC-histidine adduct on the ligating histidine in $TtCu_A$ is also removed over the course of 48 h at room temperature. The data are corroborated by electrochemical evidence showing that the 73-mV increase in reduction potential induced by DEPC modification begins reversing after 24 h of reaction. There was less loss observed using the voltammetric measurements, likely because the incubation of the modified proteins was done at 5 °C instead of room temperature.

Our spectroscopic data suggest that one ligating histidine (His157) is modified by DEPC and that the extent of modification increases with increasing pH. Considering the literature on *Tt*Cu_A, it should be noted that the N^{δ} atom on each ligating histidine participates in a coordinate covalent bond to a copper ion and remains bound at all pH values [13]. Because the N^{δ} atom is unavailable to act as a nucleophile, the N^{ε} atom must be reacting with DEPC. The ligating histidines in *Tt*Cu_A have a pK_a greater than 12 for the neutral to imidazolate transition [13], so for experiments at pH 5–9, only a tiny fraction of N^{ε} atoms are deprotonated and available to react. However, we still observe modification of a ligating histidine in this pH range. To explain this reactivity, we propose that a fast kinetic exchange of protons between N^{ε} of His157 and the solvent allows a transiently deprotonated nitrogen to react with available DEPC, overcoming the thermodynamic un-favorability of the reaction. Previous ^{1}H-NMR characterization of *Tt*Cu_A supports fast exchange of the $N^{\varepsilon}H$ proton on His157 [13], allowing for reactive ligating histidines at physiologically relevant pH values. Thus we propose that DEPC modification of a ligating histidine in *Tt*Cu_A is kinetically controlled, in contrast to the thermodynamically favorable mechanism of modification in trunc*Tt*Rp, which is facilitated by the lowered pK_a values of its ligating histidines and its corresponding pH-dependent reduction potential [17, 57, 58].

The mechanisms of DEPC modification of ligating histidines in *Tt*Cu_A and trunc*Tt*Rp are likely different, but the DEPC experiments using *Tt*Sco and azurin indicate that not every ligating histidine in a metalloprotein is reactive toward DEPC. This result implies that there are specific factors that tune the reactivity of the ligating histidines in metal centers. Solvent exposure is necessary to provide DEPC with physical access to the ligating histidines, but the degree of exposure required remains unknown. The ligating His157 in *Tt*Cu_A has a solvent exposure of nearly 23% (in the holo form) and the two ligating histidines in trunc*Tt*Rp have solvent exposure between 20 and 50%, based on GetArea [33] calculations on the respective crystal structures. The ligating His117 in azurin is only 5% exposed, whereas His139 in apo *Tt*Sco has 13% exposure. However, the accessibility of His139 likely decreases significantly upon metal binding, based on a similar analysis for known structures of other Sco proteins. From this information, it appears that ligating histidines in *Tt*Sco and azurin may not be sufficiently solvent-exposed for modification by DEPC. We also examined a mutant of azurin, F114A, which increases the solvent accessibility of a ligating histidine up to 9.7%, but without any improvement in reactivity. However, apo *Tt*Cu_A has all four of its histidines modified, including His114, which is only 3% solvent exposed in the apo form (determined using the same treatment). This result indicates that a rather low solvent exposure is sufficient for reactivity and/or perhaps that these calculations do not always reflect the true solvent accessibility of ligating histidines. If the threshold is indeed so low, then F114A azurin, if not wild-type azurin and *Tt*Sco, would potentially contain a ligating histidine with sufficient solvent-accessibility for DEPC modification. In light of these findings, reactivity may require a combination of greater solvent accessibility of the histidine ligand and an optimal electronic environment, as possibly provided by the dinuclear metal centers found in both *Tt*Rieske and *Tt*Cu_A.

Our finding that the ligating histidines in both *Tt*Rieske and *Tt*Cu_A are reactive with DEPC suggests that these histidines can undergo at least transient proton exchange on time scales appropriate for chemical reactivity. Since both trunc*Tt*Rp and *Tt*Cu_A are primarily electron

transfer proteins, this suggests a probable functional significance in connecting proton exchange events with electron transfer. For *Tt*Cu_A, this leads back to a hypothesis that the reactive ligating histidine may be involved in proton-coupled electron (PCET) transfer in Cyt*c*O. Cyt*c*O couples electron transfer to proton uptake to the catalytic site and proton translocation across the membrane [1, 2]. Proton translocation requires a series of sites within Cyt*c*O through which protons move stepwise in response to electron transfer [1, 2]. While most literature studies focus on the mechanism of proton uptake to the catalytic site and an unspecified proton-loading site, release of protons on the P-side is even less well understood. In the past, the possible importance of the Cu_A site to proton pumping has been proposed [59, 60]. On the other hand, it was later shown that His260 in *Rhodobacter sphaeroides* Cu_A (equivalent to His157 in *Tt*Cu_A) is not essential to proton pumping in Cyt*c*O [5]. That work found that proton pumping persisted for a mutant that lacked His260, though with a drastic decrease relative to its electron transfer activity. We would suggest that the apparent proton lability of this ligating histidine could still facilitate proton translocation, whereas absence of the histidine would decrease efficiency or promote an alternate pathway. Others have suggested that a ligating histidine plays a large role in proton-coupled electron transfer by acting to regulate changes in the center's valence state and the transfer of electrons to heme *a/b*, though these hypotheses rest on results obtained from Cu_A azurin [11]. Still, the rapid exchange of protons at a ligating histidine of the *Tt*Cu_A center, as observed in ^{1}H-NMR studies [13, 61] and probed here using DEPC modification, may contribute to proton translocation in cytochrome *c* oxidase and such a theory can be reconciled with previous literature results if there exists more than one exit pathway [62, 63]. Alternatively, proton exchange at His157 could facilitate switching between different electronic ground states at the Cu_A site to promote directional electron transfer [64].

Azurin is an electron transport protein that can interact with a variety of enzymes in vitro, although its exact role in vivo is still uncertain [65]. While it has not been demonstrated that PCET plays a direct role in the function of azurin, the effect of pH on non-ligating histidines near its active site has been shown to induce conformational changes that may determine its binding targets [65, 66]. Azurin has also been used as a model to study PCET by photoinduced oxidation of aromatic amino acid residues using metal-labeled azurin constructs [67]. There is even more uncertainty about the role for Sco than for azurin. Sco from *Bacillus subtilis* has been shown to behave like a redox protein with the ligating histidine stabilizing the Cu(II) metal bound form [68], but has not been linked to PCET.

Taken together, all of the data presented in this report show that one ligating histidine is modified by DEPC in *Tt*Cu_A which causes an increase of more than 70 mV to the reduction potential. The adduct is spontaneously removed after 24–72 h at room temperature. While both truncTtRp [17] and *Tt*Cu_A contain a reactive ligating histidine, ligating histidines are not modified by DEPC in *Tt*Sco and azurin, indicating that not all ligating histidines are necessarily reactive toward small molecules like DEPC. We hypothesize that the reactivity of a ligating histidine in *Tt*Cu_A specifically arises from rapid exchange of protons with the solvent, which allows it to react with DEPC. Thus, these reactive ligating histidines may have functional significance including suitability for proton translocation.

Supplementary Material

Refer to Web version on PubMed Central for supplementary material.

Acknowledgements

The research was supported by the Arnold and Mabel Beckman Foundation Beckman Scholars Program, and by the Semmes Distinguished Scholar in Science Award from Trinity University for TD. The FASTER grant SURF-National Science Foundation DUE S-STEM Award 1153796 supported CRH, and the T. Frank and Norine R. Murchison Faculty Development Fund helped support both ZA and CRH. The Berry College Faculty Development Program helped support KRH. The Trinity University Chemistry Department also helped support the work. We are grateful to the laboratory of Prof. Brian R. Crane for the plasmid used to express azurin, and to the late Jim Fee for the *Tt*Sco plasmid. We would also like to acknowledge the work of the Biochemistry Lab Students from Fall 2014 at Trinity University. The students performed the initial studies with fewer equivalents of DEPC reacting with $TtCu_A$, which led to the study performed in Fig. 4, and was described in a book chapter on integrating research and teaching [69].

References

1. Wikström M, Sharma V, Kaila VR, Hosier JP, Hummer G (2015) Chem Rev 115:2196–2221 [PubMed: 25694135]
2. Kaila VR, Verkhovsky MI, Wikstrom M (2010) Chem Rev 110:7062–7081 [PubMed: 21053971]
3. Kannt A, Soulimane T, Buse G, Becker A, Bamberg E, Michel H (1998) FEBS Lett 434:17–22 [PubMed: 9738443]
4. Xie X, Gorelsky SI, Sarangi R, Garner DK, Hwang HJ, Hodgson KO, Hedman B, Lu Y, Solomon EI (2008) J Am Chem Soc 130:5194–5205 [PubMed: 18348522]
5. Zhen Y, Schmidt B, Kang UG, Antholine W, Ferguson-Miller S (2002) Biochemistry 41:2288–2297 [PubMed: 11841221]
6. Robinson H, Ang MC, Gao Y, Hay MT, Lu Y, Wang AHJ (1999) Biochemistry 38:5677–5683 [PubMed: 10231517]
7. Williams PA, Blackburn NJ, Sanders D, Bellamy H, Stura EA, Fee JA, McRee DE (1999) Nat Struct Biol 6:509–516 [PubMed: 10360350]
8. Fee JA, Sanders D, Slutter CE, Doan PE, Aasa R, Karpefors M, Vanngard T (1995) Biochem Biophys Res Commun 212:77–83 [PubMed: 7612020]
9. Slutter CE, Sanders D, Wittung P, Malmström BG, Aasa R, Richards JH, Gray HB, Fee JA (1996) Biochemistry 35:3387–3395 [PubMed: 8639488]
10. Hay M, Richards JH, Lu Y (1996) Proc Nat Acad Sci U S A 93:461–464
11. Hwang HJ, Lu Y (2004) Proc Natl Acad Sci USA 101:12842–12847 [PubMed: 15326290]
12. Sujak A, Sanghamitra NJ, Maneg O, Ludwig B, Mazumdar S (2007) Biophys J 93:2845–2851 [PubMed: 17604317]
13. Alvarez-Paggi D, Abriata LA, Murgida DH, Vila AJ (2013) Chem Commun 49:5381–5383
14. Sanghamitra NJM, Mazumdar S (2008) Biochemistry 47:1309–1318 [PubMed: 18189418]
15. Miles EW (1977) Methods Enzymol 47:431–442 [PubMed: 22021]
16. Lundblad RL (2005) Chemical reagents for protein modification. CRC Press, Boca Raton
17. Konkle ME, Elsenheimer KN, Hakala K, Robicheaux JC, Weintraub ST, Hunsicker-Wang LM (2010) Biochemistry 49:7272–7281 [PubMed: 20684561]
18. Ramirez BE, Malmström BG, Winkler JR, Gray HB (1995) Proc Natl Acad Sci USA 92:11949–11951 [PubMed: 8618820]
19. Regan JJ, Ramirez BE, Winkler JR, Gray HB, Malmström BG (1998) J Bioenerg Biomemb 30:35–39
20. Brzezinski P (1996) Biochemistry 35:5611–5615 [PubMed: 8639518]
21. Lopez LC, Mukhitov N, Euers L, Handley LD, Hamme CS, Hofman CR, Euers L, Piers A, Wadler EH, Hunsicker-Wang LM (2018) Protein Sci 27:1942–1954 [PubMed: 30168216]
22. Edelhoch H (1967) Biochemistry 6:1948–1954 [PubMed: 6049437]

23. Pace CN, Vajdos F, Fee L, Grimsley G, Gray T (1995) Protein Sci 4:2411–2423 [PubMed: 8563639]
24. Chang TK, Iverson SA, Rodrigues CG, Kiser CN, Lew AY, Germanas JP, Richards JH (1991) Proc Natl Acad Sci USA 88:1325–1329 [PubMed: 1899926]
25. Karlsson BG, Pascher T, Nordling M, Arvidsson RH, Lundberg LG (1989) FEBS Lett 246:211–217 [PubMed: 2540038]
26. Miller JE (2003) PhD Thesis, California Institute of Technology
27. Stoll S, Schweiger A (2006) J Magn Reson 178:42–55 [PubMed: 16188474]
28. Stoll S, Britt RD (2009) Phys Chem Chem Phys 11:6614–6625 [PubMed: 19639136]
29. Jeuken LJC, McEvoy JP, Armstrong FA (2002) J Phys Chem B 106:2304–2313
30. Hoke KR, Chandler MR (2013) Chem Educ 18:263–268
31. Bard AJ, Faulkner LR (2001) Electrochemical methods: fundamentals and applications. Wiley, New York
32. Fourmond V, Hoke K, Heering HA, Baffert C, Leroux F, Bertrand P, Léger C (2009) Bioelectrochemistry 76:141–147 [PubMed: 19328046]
33. Fraczkiewicz R, Braun W (1998) J Comput Chem 19:319–333
34. Zaballa M, Abriata LA, Donaire A, Vila AJ (2012) Proc Natl Acad Sci USA 109:9254–9259 [PubMed: 22645370]
35. Abriata LA, Banci L, Bertini I, Ciofi-Baffoni S, Gkazonis P, Spyroulias GA, Vial AJ, Wang S (2008) Nat Chem Biol 4:599–601 [PubMed: 18758441]
36. Adman ET, Jensen LH (1981) Israel J Chem 21:8–12
37. Tsai LC, Sjölin T, Langer V, Pascher T, Nar H (1995) Acta Cryst D 51:168–176 [PubMed: 15299318]
38. Konkle ME, Muellner SK, Schwander AL, Dicus MM, Pokhrel R, Britt RD, Taylor AB, Hunsicker-Wang LM (2009) Biochemistry 48:9848–9857 [PubMed: 19772300]
39. Banci L, Bertini I, Calderone V, Ciofi-Baffoni S, Mangani S, Martinelli M, Palumaa P, Wang S (2006) Proc Nat Acad Sci USA 103:8595–8600 [PubMed: 16735468]
40. Abajian C, Rosenzweig AC (2006) J Biol Inorg Chem 11:459–466 [PubMed: 16570183]
41. Grace ME, Loosemore MJ, Semmel ML, Pratt RF (1980) J Am Chem Soc 102:6784–6789
42. Loosemore MJ, Pratt RF (1976) FEBS Lett 72:155–158 [PubMed: 1001460]
43. Melchior WB, Fahrney D (1970) Biochemistry 9:251–258 [PubMed: 4904867]
44. Immoos C, Hill MG, Sanders D, Fee JA, Slutter CE, Richards JH, Gray HB (1996) J Biol Inorg Chem 1:529–531
45. Hill BC, Andrews D (2012) Biochim Biophys Acta Bioenerg 1817:948–954
46. Williams JC, Sue C, Banting GS, Yang H, Glerum DM, Hendrickson WA, Schon EA (2005) J Biol Chem 280:15202–15211 [PubMed: 15659396]
47. Imriskova-Sosova I, Andrews D, Yam K, Davidson D, Yachnin B, Hill BC (2005) Biochemistry 44:16949–16956 [PubMed: 16363808]
48. Banci L, Bertini I, Cavallaro G, Rosato A (2007) J Proteome Res 6:1568–1579 [PubMed: 17300187]
49. Leary SC (2010) Antioxid Redox Signal 13:1403–1416 [PubMed: 20136502]
50. Siluvai GS, Mayfield M, Nilges MJ, Debeer George S, Blackburn NJ (2010) J Am Chem Soc 132:5215–5226 [PubMed: 20232870]
51. Pascher T, Bergström J, Malmström BG, Vänngård T, Lundberg LG (1989) FEBS Lett 258:266–268 [PubMed: 2557238]
52. Hwang HJ, Berry SM, Nilges MJ, Lu Y (2005) J Am Chem Soc 127:7274–7275 [PubMed: 15898751]
53. Ainscough EW, Bingham AG, Brodie AM, Ellis WR, Gray HB, Loehr TM, Plowman JE, Norris GE, Baker EN (1987) Biochemistry 26:71–82 [PubMed: 3030404]
54. Jackman MP, Lim MC, Osvath P, De Silva D, Sykes AG (1988) Inorg Chim Acta 153:205–208
55. Li SY, Oyala PH, Britt RD, Weintraub ST, Hunsicker-Wang LM (2017) J Biol Inorg Chem 22:545–557 [PubMed: 28197737]

56. Burstein Y, Walsh KA, Neurath H (1974) Biochemistry 13:205–210 [PubMed: 4808703]
57. Zu Y, Fee JA, Hirst J (2001) J Am Chem Soc 123:9906–9907 [PubMed: 11583559]
58. Hsueh K, Westler WM, Markley JL (2010) J Am Chem Soc 132:7908–7918 [PubMed: 20496909]
59. Nilsson T, Gelles J, Li PM, Chan SI (1988) Biochemistry 27:296–301 [PubMed: 2831955]
60. Capitanio N, Capitanio G, Minuto M, De Nitto E, Palese LL, Nicholls P, Papa S (2000) Biochemistry 39:6373–6379 [PubMed: 10828951]
61. Bertini I, Bren KL, Clemente A, Fee JA, Gray HB, Luchinat C, Malmström BG, Richards JH, Sanders D, Slutter CE (1996) J Am Chem Soc 118:11658–11659
62. Sugitani R, Stuchebrukhov AA (2009) Biochim Biophys Acta 1787:1140–1150 [PubMed: 19393218]
63. Yang L, Skjevik AA, Du Han WG, Noodleman L, Walker RC, Gotz AW (2016) Biochim Biophys Acta 1857:1594–1606 [PubMed: 27317965]
64. Abriata LA, Alvarez-Paggi D, Ledesma GN, Blackburn NJ, Vila AJ, Murgida DH (2012) Proc Natl Acad Sci USA 109:17348–17353 [PubMed: 23054836]
65. Ullmann RT, Ullmann GM (2011) J Phys Chem B 115:10346–10359 [PubMed: 21774518]
66. Nar H, Messerschmidt A, Huber R, van de Kamp M, Canters GW (1991) J Mol Biol 221:765–772 [PubMed: 1942029]
67. Warren JJ, Shafaat OS, Winkler JR, Gray HB (2016) J Biol Inorg Chem 21:113–119 [PubMed: 26790882]
68. Siluvai GS, Nakano MM, Mayfield M, Nilges MJ, Blackburn NJ (2009) Biochemistry 48:12133–12144 [PubMed: 19921776]
69. Hunsicker-Wang L, Konkle ME (2018) Best practices for supporting and expanding undergraduate research in chemistry American Chemical Society, Washington, DC, pp 165–179

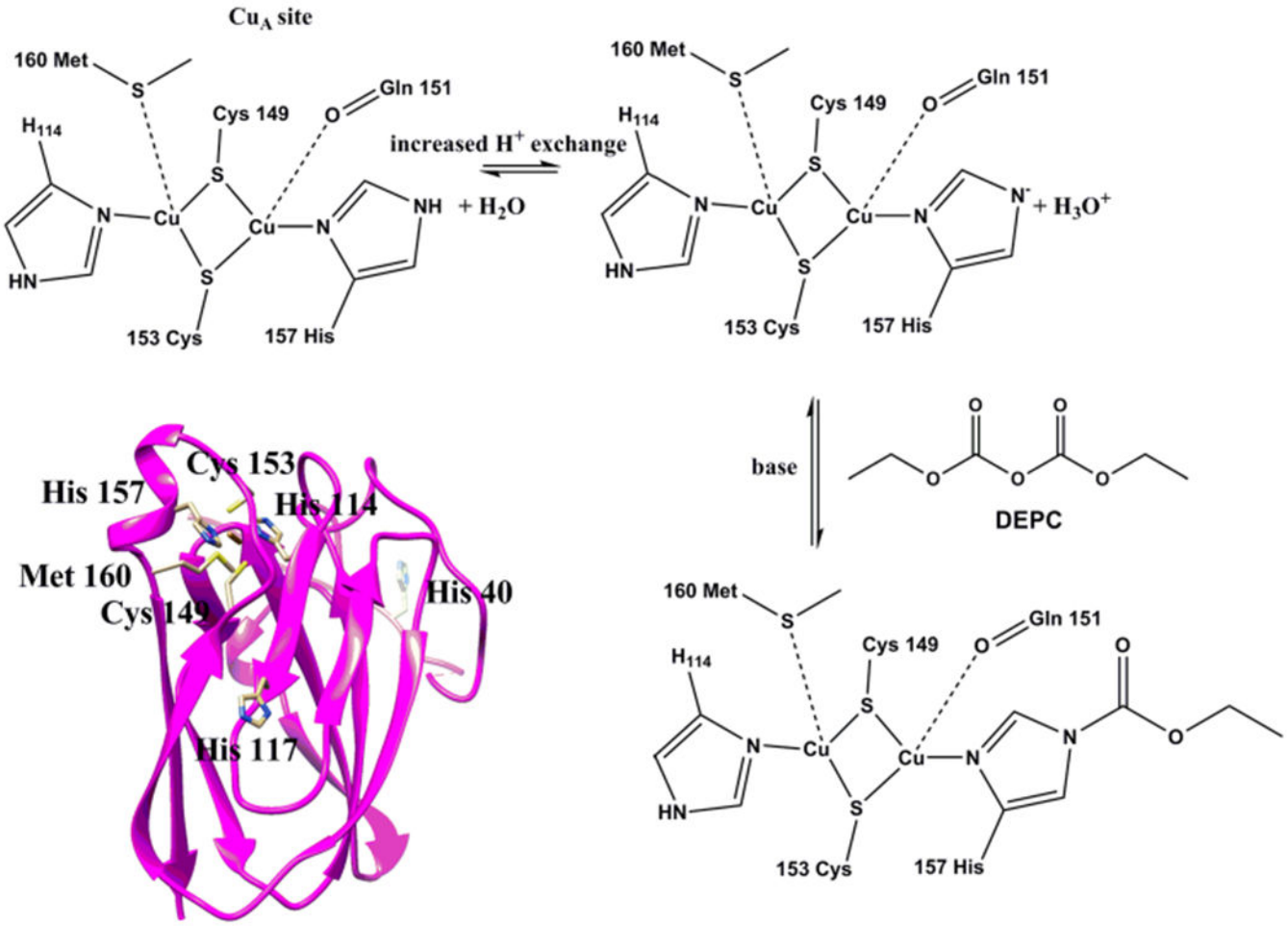

Fig. 1.

*Tt*Cu$_A$ protein, metal center, and DEPC reaction scheme. The *Thermus thermophilus* Cu$_A$ protein ribbon diagram (2CUA) (bottom, left) with ligands and all histidines shown as sticks. The Cu$_A$ metal center (top, left) and the reaction between DEPC and the more solvent exposed histidine (157) is indicated (bottom, right)

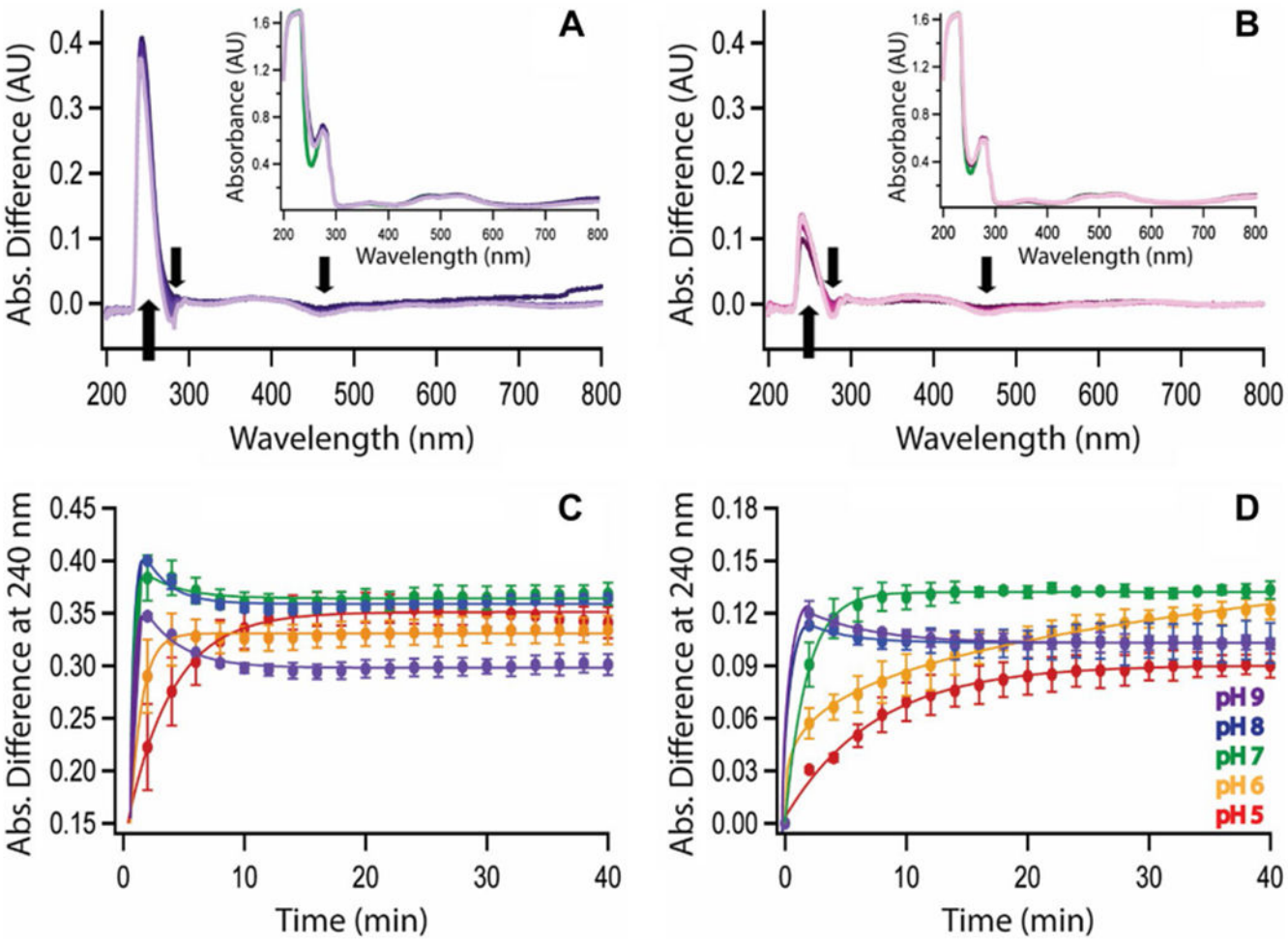

Fig. 2.

DEPC modification of **a** *Tt*Cu_A in purple and **b** H40A/H117A in pink, monitored by UV–visible spectroscopy at pH 7.0. UV–visible difference spectra were recorded from 200 to 800 nm for 40 min. Earlier scans are darker in color, and later scans are lighter in color. The arrows indicate the characteristic increase in absorbance at 240 nm due to the formation of the DEPC-histidine adduct and changes in the charge transfer bands. Each graph is representative of a triplicate run. Inset is the raw data before subtraction of the initial spectrum (green). Plot of change in absorbance at 240 nm for **c** *Tt*Cu_A and **d** H40A/H117A after addition of DEPC at pH 5.0 (red), pH 6. (orange), pH 7.0 (green), pH 8.0 (blue), and pH 9.0 (purple). Error bars are ± 1 standard deviation of triplicate measurements. Lines drawn are to guide the eye only

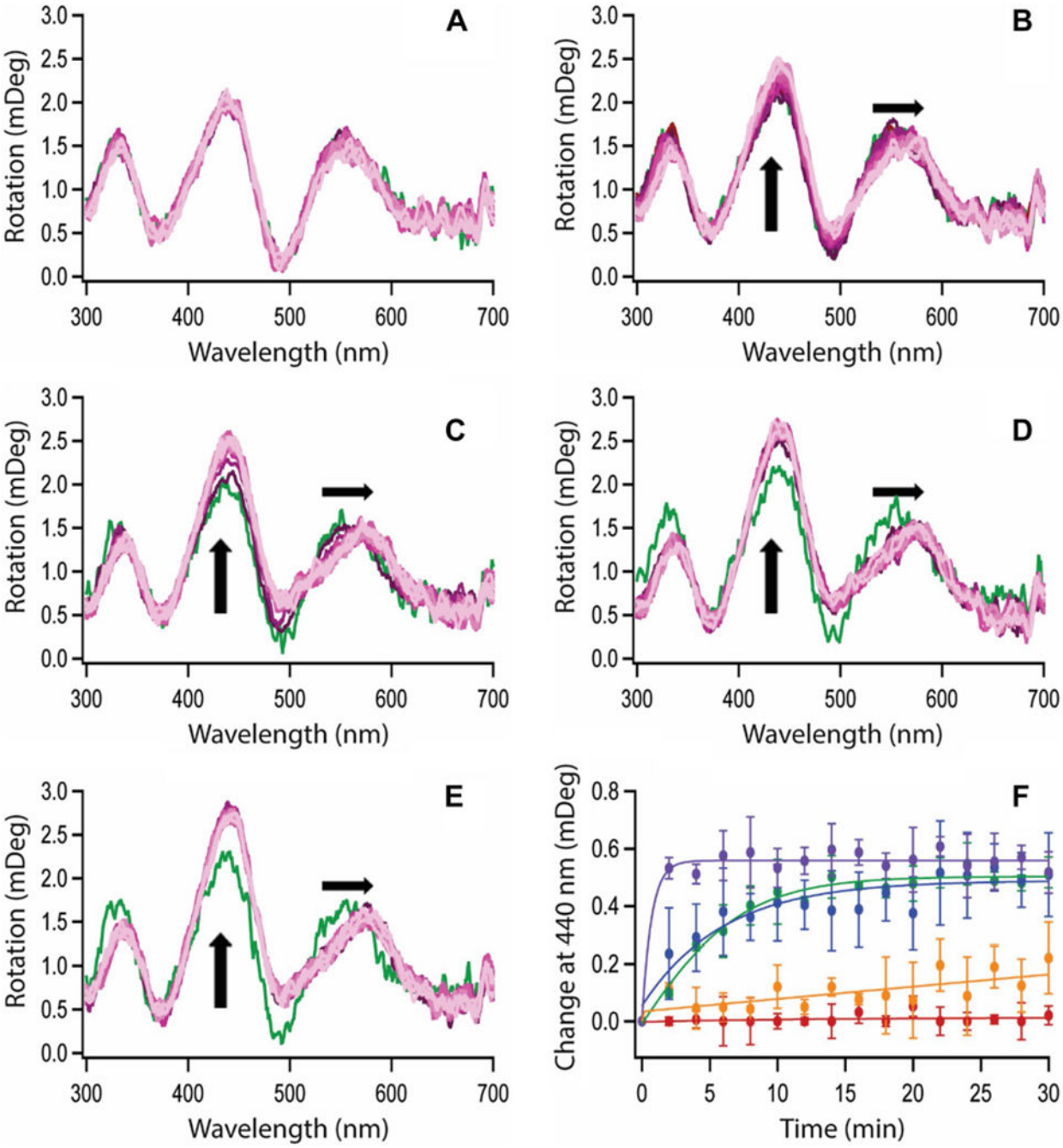

Fig. 3.

Overlaid CD spectra of H40A/H117A reacted with DEPC over 40 min at **a** pH 5.0, **b** pH 6.0, **c** pH 7.0, **d** pH 8.0, and **e** pH 9.0. Initial scans without addition of DEPC are in green. Earlier scans are darker in color, and later scans get lighter in color. Arrows indicate direction of change. Each set of spectra is representative of triplicate runs. **f** The average change in mDeg at 440 nm plotted over time at pH 5.0 (red), pH 6.0 (orange), pH 7.0 (green), pH 8.0 (blue), and pH 9.0 (purple). Error bars are ± 1 standard deviation

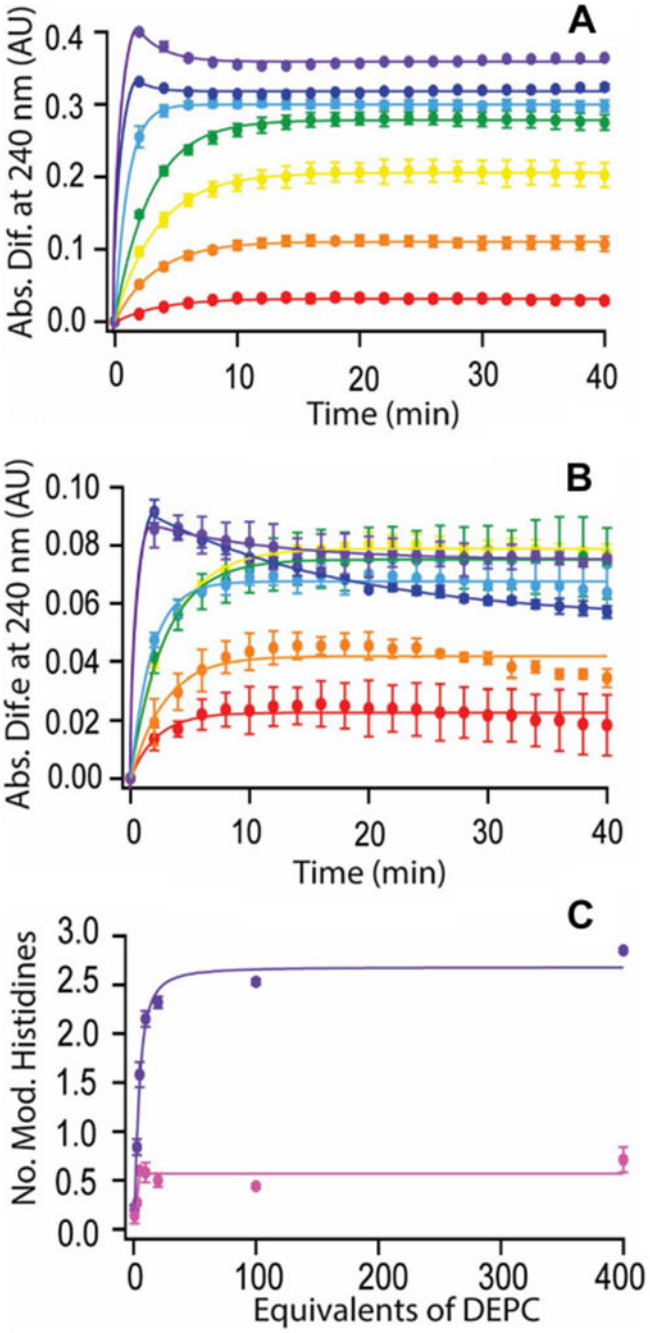

Fig. 4.

a UV–visible absorbance difference at 240 nm after the addition of 1 (red), 3 (orange), 5 (yellow), 10 (green), 20 (sky blue), 100 (dark blue), or 400 (purple) equivalents of DEPC to 40 μM *Tt*Cu_A at pH 8.0. **b** UV–visible absorbance difference at 240 nm after the addition of 1–400 equivalents of DEPC to 40 μM H40A/H117A at pH 8.0. Error bars are ± 1 standard deviation. Lines drawn are to guide the eye only. **c** Saturation curves, with fitting, for the number of modified histidines as the concentration of DEPC increases. *Tt*Cu_A is in purple and H40A/H117A is in pink

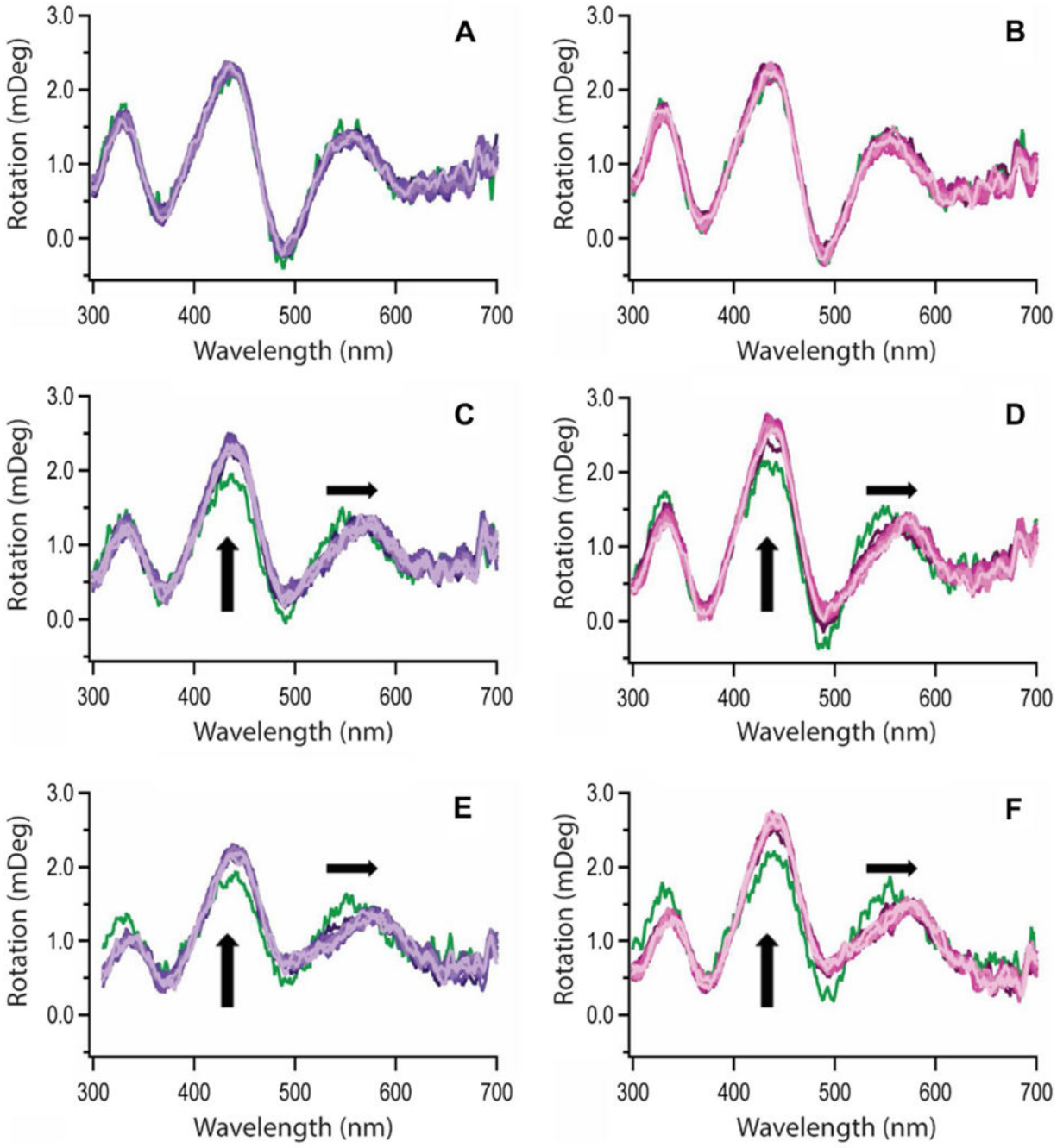

Fig. 5.

Changes to the CD spectra of *Tt*Cu_A at pH 8.0 upon the addition of **a** 1, **c** 5, or **e** 400 equivalents of DEPC and H40A/H117A after adding **b** 1, **d** 5, or **f** 400 equivalents of DEPC. Spectra were taken every 2 min for 40 min after the addition of DEPC. The initial spectrum is in green. Earlier spectra are darker in color and later spectra are lighter in color

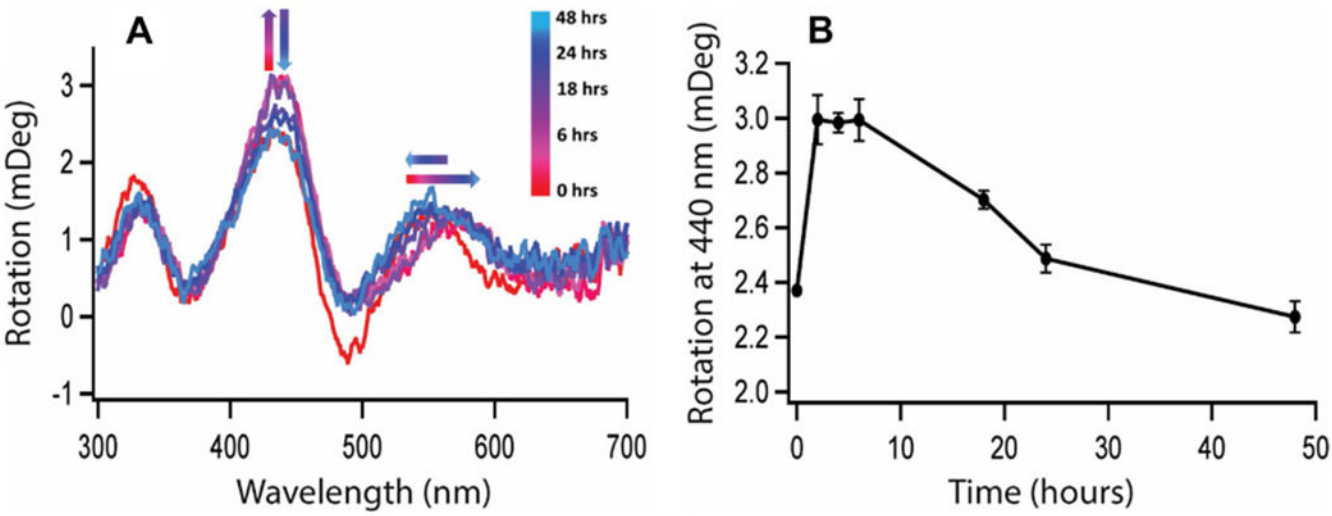

Fig. 6.

a Change to the CD spectrum of 200 μM *Tt*Cu_A at pH 8.0 up to 48 h after the addition of 400 equivalents of DEPC. Only some transitions are reversible including the increase at 440 nm and the redshift at 530 nm. **b** Plot of optical rotation at 440 nm over 48 h

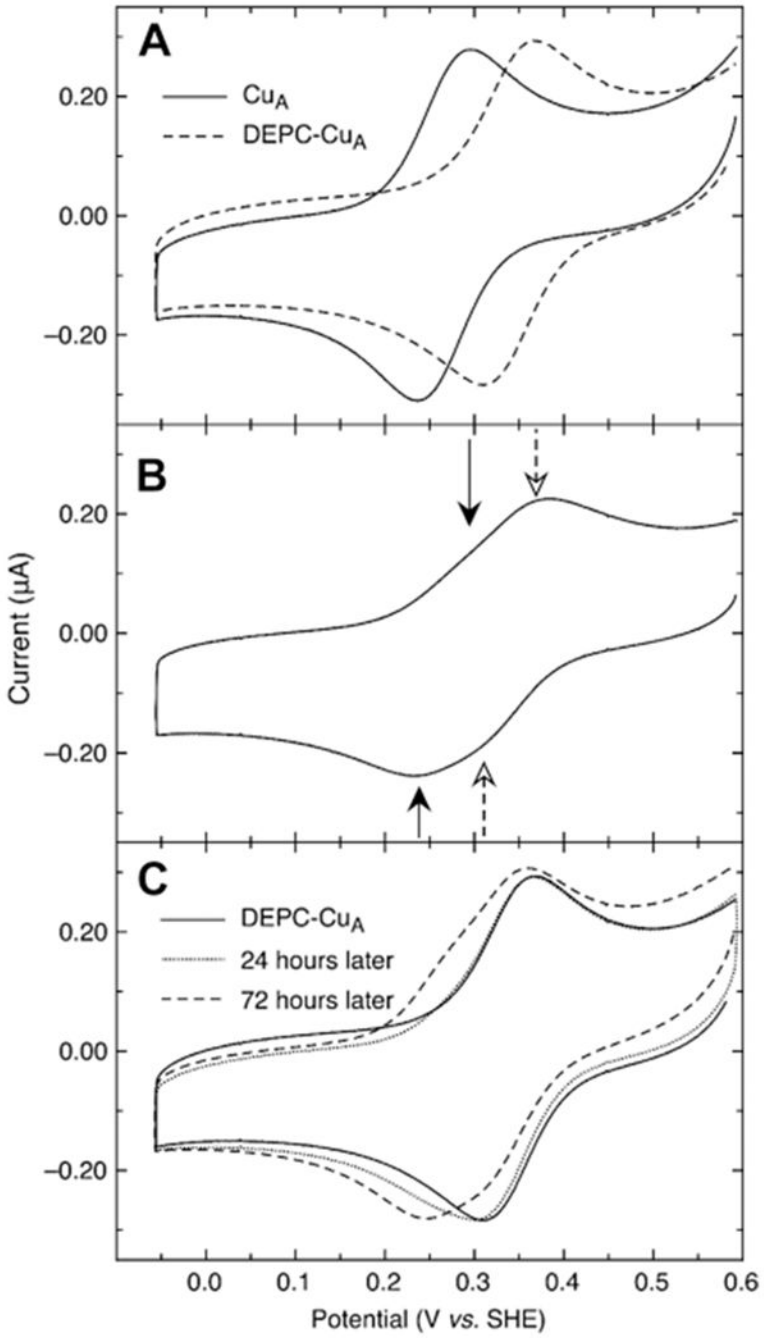

Fig. 7.

a Cyclic voltammetry of 160 μM Cu_A (solid line) and 140 μM DEPC-modified Cu_A (dashed) at 0.1 V/s in 25 mM sodium phosphate, pH 8.0. **b** One minute after mixing Cu_A with 20 equivalents of DEPC. Solid arrows denote approximate peak positions for unmodified Cu_A and dashed arrows denote the positions for DEPC-modified Cu_A. **c** Freshly prepared DEPC-modified Cu_A (solid line), then after 24 h (dotted line) and 72 h at 5 °C (dashed line)

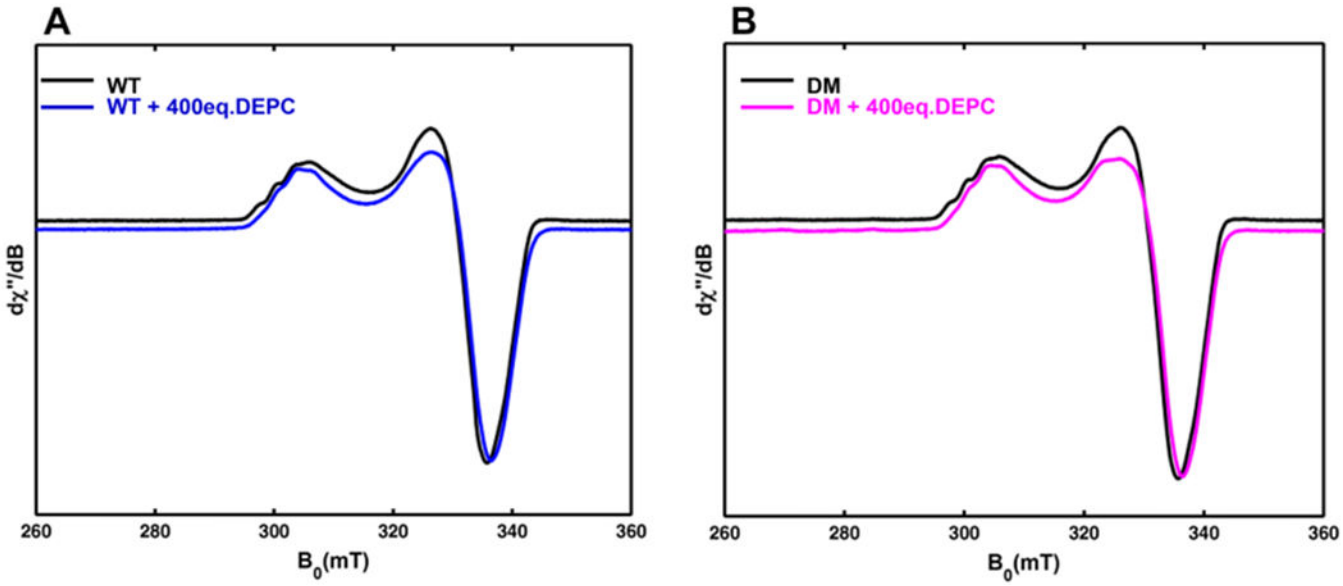

Fig. 8.

X-band CW EPR spectra of the wide-type *Tt*Cu_A (**a**) and the double-mutant (DM) H40A/H117A (**b**) with and without the addition of 400 equivalents of DEPC. Experimental parameters: temperature = 15 K; microwave frequency = 9.38 GHz; microwave power = 0.02 mW (no saturation); conversion time = 40 ms; modulation amplitude = 0.5 mT; modulation frequency = 100 kHz

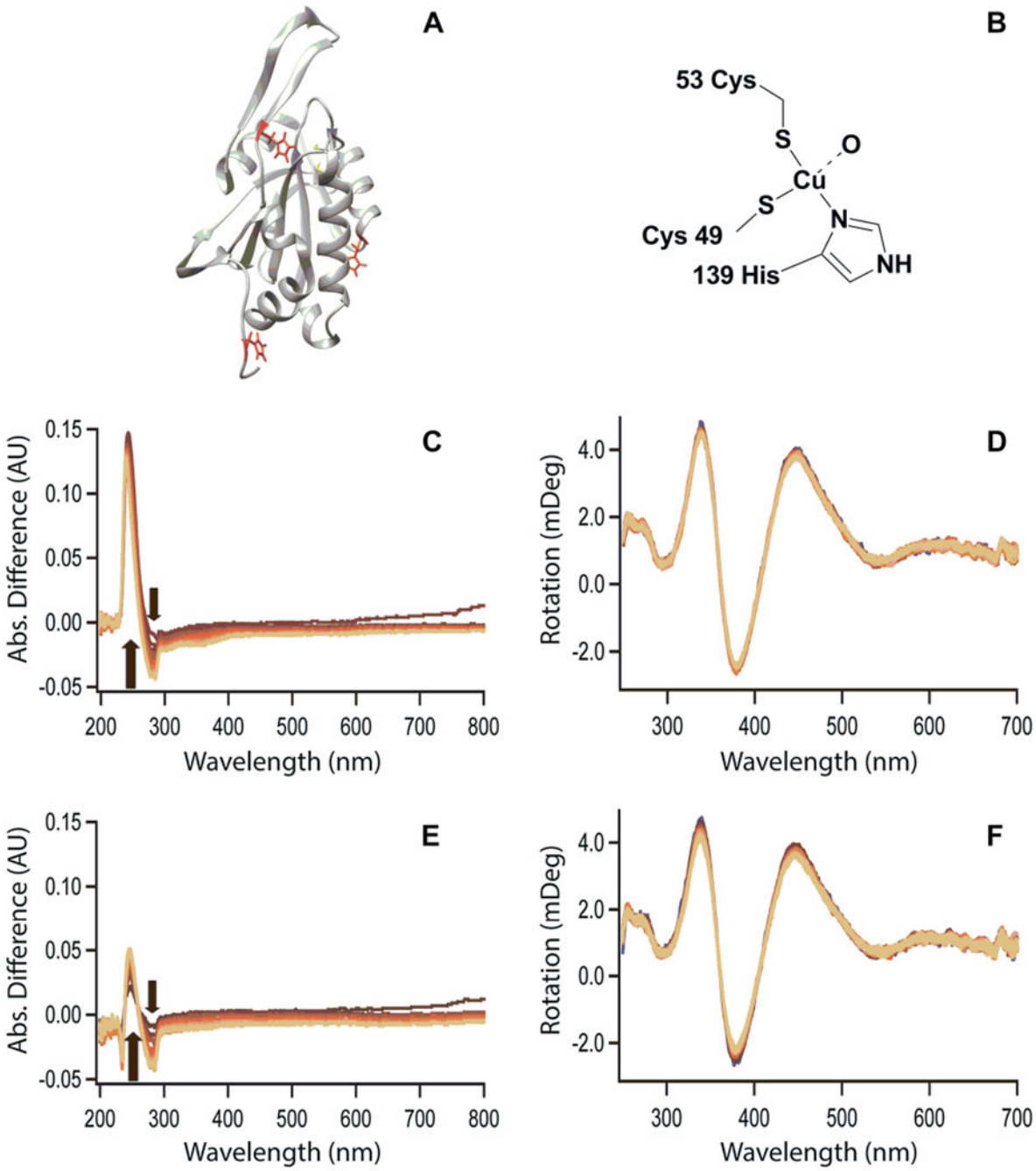

Fig. 9.

a Ribbon diagram of *Tt*Sco, **b** proposed metal binding site of the Sco protein. **c** UV–visible difference spectra of holo *Tt*Sco, **e** UV–visible difference spectra of holo H6A/H00A at pH 7.0 after addition of 400 equivalents of DEPC. All scans were taken from 200 to 800 nm every 2 min for 40 min. **d** CD spectra of 100 μM holo *Tt*Sco, **f** CD spectra of 100 μM holo H6A/H100A, after the addition of 400 equivalents of DEPC. A scan from 250 to 750 nm was taken every 2 min for 2 h. The initial scan before the addition of modifier is in blue. Earlier scans are darker in color and later scans are lighter in color

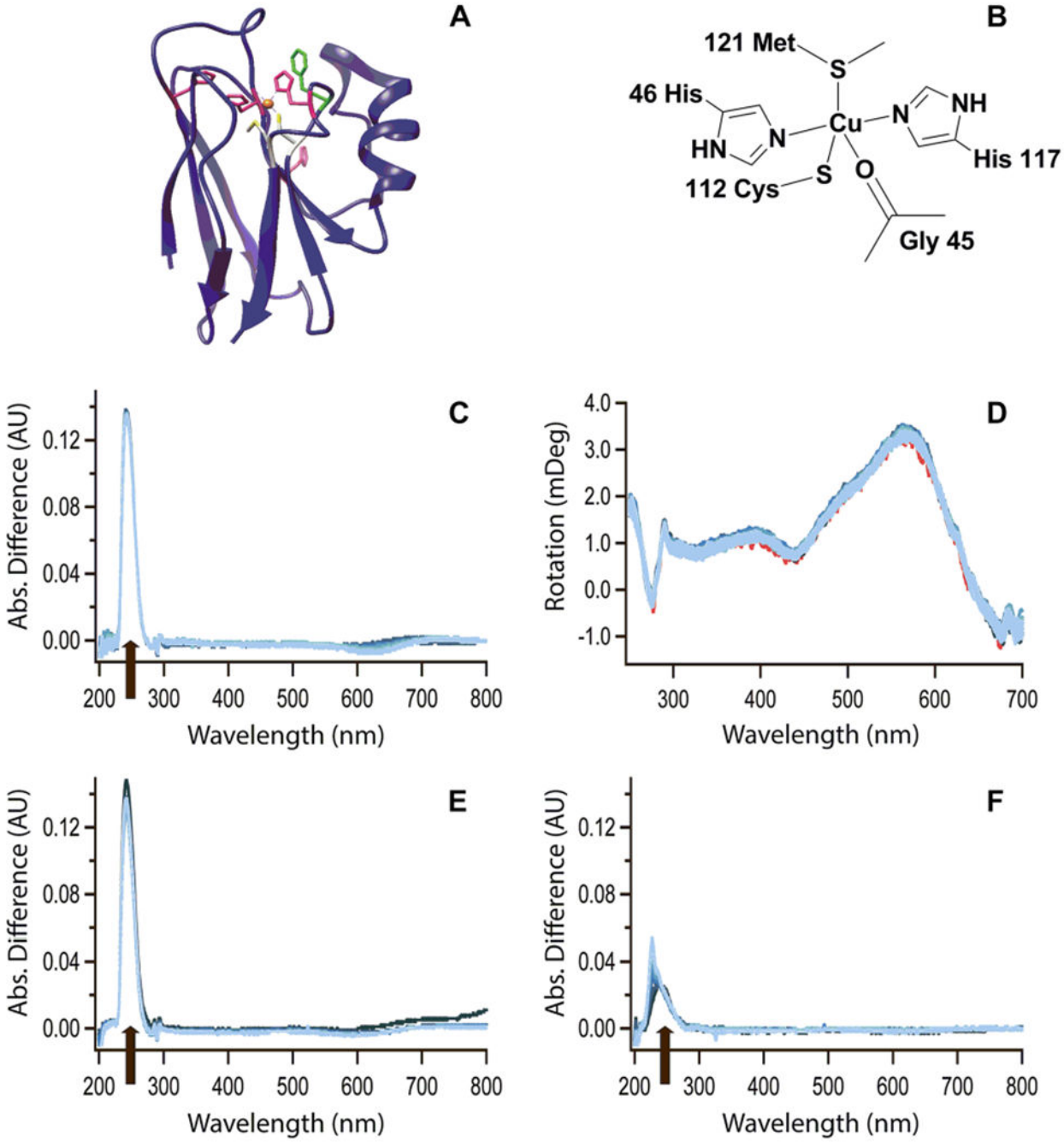

Fig. 10.

a Ribbon diagram of azurin, **b** metal site of azurin, **c** UV–visible difference spectra of wild-type azurin at pH 8.0 after the addition of 400 equivalents of DEPC. **d** CD spectra of 100 μM azurin before (red) and after the addition of 400 equivalents of DEPC. A scan from 250 to 750 nm was taken every 2 min for 2 h. Earlier scans are darker in color and later scans are lighter in color. UV–visible difference spectra of **e** F114A azurin and **f** H35A/H83A/F114A at pH 8.0 after the addition of 400 equivalents of DEPC. For all UV–visible experiments, a

scan was taken from 200 to 800 nm every 2 min for 40 min. Earlier scans are darker in color and later scans are lighter in color

Table 1

List of forward primers for all mutations

Protein	Mutation	Forward primer[a]
TtCu_A	H40A	5’ CACCCTGGCCACC**GC**CACCGCCGG 3’
	H117A	5’ GTGATCCACGGCTTT**GC**CGTGGAGGGCACC 3’
*Tt*Sco	H6A	5’ CTTCCCCGGGGG**GC**CACCTTCTACGGCAC 3’
	H100A	5’ CGCCAAGGCCTTC**GC**CCCGAGCTTCTCG 3’
Azurin	H35A	5’ CACTGTTAACCTGTCT**GC**CCCAGGTAACCTGCCG 3’
	H83A	5’ CTCGAGTTATCGCC**GC**CACCAAGCTGATCGG 3’
	F114A	5’ CATGTTCTTCTGCACT**GC**CCCGGGTCACTCCGC 3’

[a]Reverse primers are the reverse compliment of the forward primer. The changed nucleotides resulting in each point mutation are in bold and underlined

Table 2

Estimated number of modified histidines for each protein[a]

Protein	PH				
	5.0	6.0	7.0	8.0	9.0
	No. His	No. His	No. His	No. His	No. His
Holo *Tt*Cu_A[b]	2.7	2.6	2.9	2.9	2.4
Apo *Tt*Cu_A	–	–	4.0	–	–
H40A/H117A	0.7	0.9	1.0	0.7	0.8
*Tt*Sco	–	–	1.0	–	–
H6A/H100A[d]	–	–	0.4[c]	–	–
Azurin	–	–	–	1.0	–
F114A	–	–	–	1.0	–
H35A/H83A	–	–	–	0.1[c]	–
H35A/H83A/F114A	–	–	–	0.2[c]	–

[a]Determined from a triplicate experiment using the change in absorbance at 240 nm 40 min after addition of DEPC. The error on the absorbance measurements is 0.001–0.01, and the error on the calculated histidines is higher

[b]There is some apo protein found in the holo *Tt*Cu_A samples, as determined by recent ESI-TOF experiments. Thus, the estimated number of modified histidines may be somewhat overestimated for this sample

[c]Average from two replicate experiments

[d]Calculated from the maximum absorbance at 247 nm

Table 3

Calculated percentage solvent accessibilities of histidines using GetArea[a]

Protein	Residue	Solvent accessibility	
		Apo	Holo
TtCu_A	His40	–[b]	70.5[c]
	His114	2.9 (1.3–3.8)	0
	His117	25.7 (7.3–38.7)	22.9 (19.8–26)
	His157	94.5 (73.8–100)	22.5 (21.8–23.1)
*Tt*Sco	His6	55.8 (16.4–88.9)	–
	His100	8.7 (2.3–30.6)	–
	His139	12.6 (1.8–29)	–
Azurin	His35	–	0
	His46	–	0
	His83	–	52.3
	His117	–	5
F114A Az	His35	–	0
	His46	–	0
	His83	–	43.6 (40.4–49)
	His117	–	7.4 (5.9–9.7)
*Tt*Rieske[d]	His134	–	23.2 (23.1–23.3)
	His154	–	50.8 (50.7–50.8)

[a] If more than one chain exists in the file, the solvent accessibility is given as an average and range

[b] Not available in the structure

[c] Only modeled in chain B

[d] Data from chain A [38]